ESTABLISHMENT OF SELENODETIC CONTROL THROUGH MEASUREMENTS ON THE LUNAR SURFACE

Robert McLean

ESTABLISHMENT OF SELENODETIC CONTROL THROUGH MEASUREMENTS ON THE LUNAR SURFACE

A Thesis

Presented in Partial Fulfillment of the Requirements
for the Degree Master of Science

by

Robert McLean, B. S.

The Ohio State University
1970

Approved by

_____

Advisor
Department of Geodetic Science

ACKNOWLEDGMENT

The author expresses his appreciation to Professor Ivan I. Mueller for suggesting this area of research, and acknowledges the many helpful suggestions received from him.

My appreciation is also extended to the Mapping Sciences Laboratory of the National Aeronautics and Space Administration for their interest in this work, and their invaluable assistance. (Contract No. NAS 9-9695).

The author is grateful to Mrs. Evelyn Rist for the noticeably excellent typing of this thesis and to Messrs. Haim Papo and Francis Fajemirokun for their comments on the manuscript.

Special appreciation is extended to the author's wife, Mary Ann, for her patience and encouragement during this study.

Finally, it is a pleasure to express appreciation to the United States Navy for giving me the opportunity to study the science of geodesy.

TABLE OF CONTENTS

LIST OF FIGURES

LIST OF TABLES

1. INTRODUCTION

The purpose of this paper is to investigate and recommend suitable types of measurements on the lunar surface which will result in the establishment of a selenodetic control network. In this paper, we will define a selenocentric celestial coordinate system, in which we may make measurements, and in turn determine an astronomic position on the lunar surface. Combining this astronomic position with a knowledge of the deflection of the vertical at this position, we could then determine the coordinate of this position in a selenographic system.

Therefore this paper will be divided into two primary areas which are:

(1) Establishment of a selenocentric celestial coordinate system and measurements in that system from the lunar surface.

(2) Determination of the deflections of the vertical on the lunar surface.

2. ESTABLISHMENT OF AND MEASUREMENTS IN THE LUNAR ASTRONOMICAL COORDINATE SYSTEMS

On the earth most of the geodetic astronomic calculations are made using a geoequatorial system where the star coordinates are right ascension and declination. There are a great number of catalogs, maps and almanacs giving the coordinates of the stars and other celestial bodies in this system. If the coordinates in this system could be easily transformed to a lunar equatorial system, all the methods of geodetic astronomy could be employed on the moon for selenodetic purposes. In this section we will show such a transformation complete with error analysis, while also discussing such related factors as time, location of lunar pole stars and observations in the horizon system.

We will also show some methods which may be used on the lunar surface to determine astronomic position. These methods will be discussed in relation to the instrument requirements, and accuracy of the system as a whole. Included among these methods is an inertial system, which is presently installed on the lunar module, and which in itself can establish a position on the lunar surface.

The methods and instruments presented are not assumed to be a complete listing, but are based on practical factors which may obviously limit other methods because of physical size or complexity of equipment, time required to achieve an astronomic position, or excessive burden being placed on the astronauts, either during training or during the operation itself. In this light we would most like to find a method which is as conservative of the astronauts time as possible (in both training and employment), achieves satisfactory results, and does not involve undue calculations or recording procedures. In conjunction, we wish the instruments involved in this method to be simple, portable, and of course accurate.

2.1 Lunar Astronomy

Kolaczek [14] defines a selenoequatorial coordinate system (lunar right ascension system) where the axis of rotation of the moon defines the celestial pole, which is the basic direction, and the celestial equator, which is a plane perpendicular to the rotation axis, containing the center. The latter is defined as the basic plane. This system is affected by precession and nutation (physical libration) of the lunar axis of rotation. The selenoequatorial system is analogous to the geoequatorial system on earth, but the selenoequatorial coordinates of the stars change their values faster than the geoequatorial coordinates due to the lunar precession being 1,360 times faster than the earth's. The selenoequatorial coordinates are:

α^{Ω} - Lunar right ascension measured on the lunar celestial equator from its ascending node on the ecliptic. It is measured to the east from 0° to 360°.

d - Lunar declination which is the angular distance from the lunar celestial equator. It is measured from 0° to 90°, positive in the northern celestial hemisphere, and negative in the southern.

Now we will take a coordinate system with known coordinates and transform these coordinates into the selenoequatorial coordinate system. The translation of any coordinate system from one point in space to another changes the values of the spherical coordinates of fixed points on the celestial sphere. This change is caused by the parallax or the translation of the origin of a coordinate system and the aberration caused by the different motion of this newly translated system. The translation of mean earth oriented coordinates into mean lunar oriented coordinates does not require consideration of parallax if we consider only the coordinates of stars, as we may omit the parallax of the earth-moon distance, due to the great distance of the stars, as compared to the earth-moon distance. The transformation of the apparent coordinates however requires consideration of the influence of the moon's aberrations.

2.1.1 Transformation of Mean Geoequatorial into Mean Selenoequatorial Coordinates

The transformation of mean geoequatorial into mean selenoequatorial coordinates can be performed in two steps [14]. First the mean geoequatorial coordinates α, δ are transformed into the mean ecliptic coordinates λ, β by the well known formulas:

$$\sin\beta = \cos\epsilon \sin\delta - \sin\epsilon \cos\delta \sin\alpha$$

$$\cos\beta \cos\lambda = \cos\delta \cos\alpha$$

$$\cos\beta \sin\lambda = \sin\epsilon \sin\delta + \cos\epsilon \cos\delta \sin\alpha$$

where ϵ the obliquity of the ecliptic is

$$\epsilon = 23^\circ.452294 - 0^\circ.0130125\ T - 0^\circ.00000164\ T^2 + 0^\circ.000000503\ T^3$$

where T denotes the time measured in Julian centuries of 36,525 ephemeris days from the epoch 1900 January 0.5ET = J.D. 2415020.0.

Next the transformation formulas of mean ecliptic coordinates into mean selenoequatorial coordinates.

$$\left.\begin{aligned} \sin d_m &= \sin\beta \cos I + \cos\beta \sin I \sin(\lambda - \Omega) \\ \cos d_m \sin\alpha^{\Omega}_{m} &= \sin\beta \sin I - \cos\beta \cos I \sin(\lambda - \Omega) \\ \cos d_m \cos\alpha^{\Omega}_{m} &= -\cos\beta \cos(\lambda - \Omega) \end{aligned}\right\} \quad 2.1$$

where I is inclination of the lunar equator to the ecliptic

$$I = 1^\circ\ 32'\ 01''$$

Ω The mean longitude of the ascending node of the lunar orbit on the ecliptic is

$$\Omega = 259^\circ.18305556 - 1934^\circ.14200833\ T + 0^\circ.002078\ T^2 + 0^\circ.000002\ T^3$$

where T is defined as above.

2.1.2 Transformation of Mean Selenoequatorial Into Apparent Selenoequatorial Coordinates

The transformation of mean into apparent coordinates is given in a form [14] similar to that used for the earth's equatorial coordinates

$$\alpha^{\Omega}_{sapp} = \alpha^{\Omega}_{m} + A_1 a_1 + B_1 b_1 + C_1 c_1 + D_1 d_1 + \tau_a \mu_a$$

$$d_{sapp} = d_m + A_1 a_1' + B_1 b_1' + C_1 c_1' + D_1 d_1' + \tau_a \mu_d$$

Similarly to Bessel's equations on the earth, A_1 and B_1 are the effects of precession and nutation to date from the determination of the mean coordinates. The C_1 and D_1 terms are the effect of lunar annual abberation. The $\tau_a \mu (d/a)$ terms are the corrections for proper motion. The $a_1, b_1, c_1, d_1, a_1', b_1', c_1', d_1'$ coefficients are the lunar Besselian star constants. Specifically:

$$A_1 = -(P_o^d t + \sigma) \sin I$$

$$B_1 = \rho$$

$$C_1 = -K \sin(L_{ap} - \Omega + 180^\circ) \cos I$$

$$D_1 = -K \cos(L_{ap} - \Omega + 180^\circ)$$

where:

P_o^d - Daily motion of the ascending node of the moon's orbit on the ecliptic ($= -0^\circ.0529539222$)

t - Number of ephermeris days from the epoch t_o of the mean coordinates $\alpha \; \Omega_\mathbb{D}, d_m$

I - Inclination of the moon's equator to the ecliptic ($=1^\circ\ 32'\ 01''$)

ρ, σ - Physical librations in inclination and in ascending node respectively (see Appendix #3)

K, k - Constant of the earth's and of the lunar aberration respectively

$K = k(1 - V_1 \cos(L_s - l_1)/V_e)$

($k = 20''.4958$)

L_s, l_1, L_{ap} - Longitude of the sun, the moon and the moon's apex in the motion around the sun respectively

$L_{ap} = L_S - 90^\circ + \Delta A$

$$\Delta A = \tan^{-1}\left(\frac{V_l \sin(L_s - l_l)}{V_e - V_l \cos(L_s - l_l)}\right)$$

V_e, V_l - Velocity of the earth's and the moon's orbital motion, respectively

(V_e = 29.8 km/sec

V_l = 1.02 km/sec)

The lunar Besselian star constants are:

$$a_l = (\cot I - \sin \alpha_m^{\Omega} \tan d_m)$$
$$a_l' = -\cos \alpha_m^{\Omega}$$
$$b_l = \cos \alpha_m^{\Omega} \tan d_m$$
$$b_l' = -\sin \alpha_m^{\Omega}$$
$$c_l = -\cos \alpha_m^{\Omega} \sec d_m$$
$$c_l' = \sin \alpha_m^{\Omega} \sin d_m + \tan I \cos d_m$$
$$d_l = \sin \alpha_m^{\Omega} \sec d_m$$
$$d_l' = \cos \alpha_m^{\Omega} \sin d_m$$

The proper motion will take on similar values to those computed on the earth:

$\tau_a = t$

μ_a, μ_d = The components of proper motion of the star

2.1.3 Lunar Horizon System

Measurements on the lunar surface will most likely be made in the horizon system. In the moon's horizon system, altitude a_{lh} and azimuth A_{lh} are defined in the same way as that of the earth's horizon system. The transformation between the lunar horizon system and the lunar selenoequatorial system similar to that given by Mueller [16] is as follows:

$$\left.\begin{aligned} \cos d \sin(LHA_{\Omega} - \lambda - \alpha^{\Omega}) &= -\sin Z_l \sin A_{lh} \\ \sin d &= \cos Z_l \sin\Phi + \sin Z_l \cos A \cos\Phi \\ \cos d \cos(LHA_{\Omega} - \lambda - \alpha^{\Omega}) &= \cos Z_l \cos\Phi - \sin Z_l \cos A_{lh} \sin\Phi \end{aligned}\right\} 2.2$$

where LHA_{Ω} - The lunar hour angle of the node measured from the reference median

Φ - The lunar astronomical latitude

λ - The lunar astronomical longitude

$Z_1 = 90 - a_{1h}$

The above equations can be derived with the use of Figure 1 below:

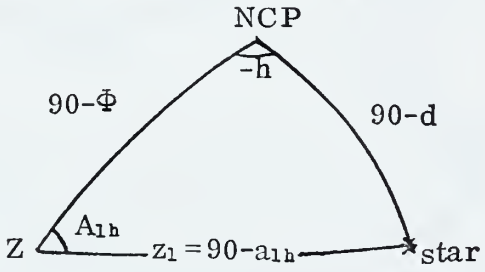

$$h = LHA_{\Omega} - \lambda - \alpha^{\Omega}$$

Figure 1. - The Astronomical Triangle

2.2 Lunar Time

As we have defined the lunar right ascension system in terms of ascending node, it would only be appropriate, that we define the lunar time system in terms of the draconic month. The draconic month is defined by two successive passages of the moon through the same node of its orbit. The draconic month is equal to 27.212220 mean solar days.

The expression of selenographic longitude in terms of time would be as follows:

1 month	=	27.212220	mean solar days	=	360°
1 day	=	.9070740	mean solar days	=	12°
1 hour	=	.03779475	mean solar days	=	30'
1 minute	=	.0006299125	mean solar days	=	30"
1 second	=	.0000104985	mean solar days	=	0".5

Figure 2 below shows the relationship in draconic times.

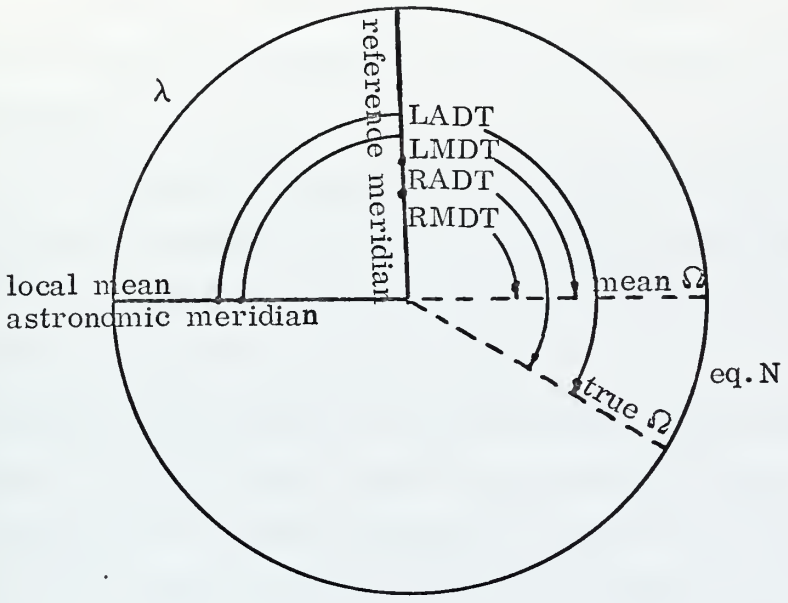

LMDT	Lunar mean draconic time
LADT	Lunar apparent draconic time
RMDT	Reference mean draconic time
RADT	Reference apparent draconic time
eq.N	Equation of the node

Figure 2. - Draconic Time System

From Figure 2 it is evident that:

$$LMDT + eq.N = LADT$$

and $$LMDT - RMDT = \lambda$$

where λ - The reduced astronomic longitude with the positive sign to the east

and eq.N - The lunar equation of the node which is due to nutation (physical libration in longitude τ and in node σ) (see Appendix C).

From the actual rotation angles of the moon, we find that eq.N = $\tau - \sigma$.

We will assume in this section that the meridian is not affected by polar motion and that the rotation of the moon is free from short periodic irregularities.

The hour angle of the node is equal to the lunar right ascension of an object at the instant of its upper transit over the meridian from which the hour angle is reckoned. Therefore, draconic time can be determined by observing transits of stars.

The lunar time intervals are almost equal to the terrestrial time intervals of the same name (91% of the terrestrial values), which is still advantageous from the psychological point of view because a change to such a time system would be almost unnoticeable to man. The meridian to use for a change of dates could be the 180° meridian.

2.3 Lunar Pole Stars

As stated by Gurevich [5] the lunar poles describe circles in the celestial sphere with an angular diameter of 3° . This circle is centered on the ecliptic pole, with a period of 18.6 years. Therefore, first certain stars, then others, will be most suited for use as pole stars. Tables of altitudes and azimuths must be compiled for the stars closest to the poles at a particular time. The mean north pole of the moon described in the earth right ascension system would be approximately, $\alpha = 18_h$, $\delta = 66°33'$. We see from the FK4 catalogue that the following stars from Table 1 are near the north pole.

Table 1. Lunar North Pole Stars

Catalog Number	Magnitude	α	δ
659	5.21	$17^h\ 32^m$	$68^\circ\ 09'$
701	6.00	$18^h\ 36^m$	$65^\circ\ 27'$
664	4.87	$17^h\ 37^m$	$68^\circ\ 46'$
685	5.03	$18^h\ 13^m$	$64^\circ\ 23'$

and approximately $\alpha = 6^h$, $\delta = -66^\circ\ 33'$ for the south pole in Table 2 from the Boss catalogue.

Table 2. Lunar South Pole Stars

Catalog Number	Magnitude	α	δ
6927	5.3	$5^h\ 32^m$	$-64^\circ\ 15'$
7246	4.5	$5^h\ 44^m$	$-65^\circ\ 45'$
7384	5.2	$5^h\ 49^m$	$-66^\circ\ 55'$
7813	5.8	$6^h\ 06^m$	$-66^\circ\ 02'$
7946	4.9	$6^h\ 11^m$	$-65^\circ\ 35'$

With a knowledge of the relationship of the position of the lunar pole to those stars the astronauts can make a rough north alignment with a probable accuracy of less than 1 minute while using only a gun sight type sighting device.

2.4 Measurements on the Lunar Surface

Presented here are four basic types of measurements which can be employed on the lunar surface to determine astronomic position.

One method is the measurement of altitudes or zenith angles of at least two stars separated in azimuth, combined with the known celestial coordinates of a star and a knowledge of time. This is a method which can be employed with an ordinary sextant or theodolite.

A second method is by determination of a relative bearing and altitude of a star combined with information from inertial and gravitational sensors, which is the method used by the Alignment Optical Telescope (AOT) on the lunar module.

A third method is by measurement of relative azimuth angles between at least three known stars. This technique can be used with an ordinary theodolite, but also lends itself well to the use of an automatic instrument.

A fourth method is by star photography, which can use either the first or third, or other methods to determine position. Here we can use a photo theodolite, or other metric camera.

In the following section these four methods will be discussed in relation to their ease of employment on the lunar surface, instrumental adaptability and accuracy, and other pertinent facts.

2.4.1 Method 1: Measurements of Altitudes

The measurement of altitudes or zenith angles in order to determine astronomical positions can be accomplished by the use of a sextant or theodolite. The obvious advantage of this method lies in the fact that both sextants and theodolites are comparatively light equipment, which could feasibly be included on a lunar mission. The sextant is a familiar instrument to the astronauts, as they already have been trained in its use. Although, the training required to allow the astronauts to effectively use a theodolite could be accomplished in a short period of time. The big

advantage in using this equipment is that astronomical positions can be taken at several points.

As stated in the Geonautics study [7], it is not likely though that a theodolite would be practicable for the initial missions. The time and effort required to set up and measure is far out of proportion to the many other tasks required of the astronauts. It would also be necessary to adapt the fine pointing and adjusting screws for use with the pressure gloves the operator must wear. In addition, precise sightings through the helmet face plate would be most difficult.

A hand held sextant may be used to determine a position on the lunar surface. The altitude of a star is read directly from the scale. With the aid of sub-divisions and a vernier, altitudes can be read with a first-class instrument to one-tenth of a minute of arc.

The problem which arises with the use of a simple sextant is in the determination of the lunar horizon. In order to eliminate this problem, we can consider the use of an artificial horizon or a bubble sextant, so that we then need only define the local vertical instead of the horizon.

The artificial horizon is a rectangular shallow basin of mercury. The observer places himself so that he can see the image of the body, whose altitude is to be measured, reflected in the mercury. He points the telescope toward the artificial horizon so that he uses a second image of the heavenly body in place of the horizon. By moving the index arm, the two images are made to coincide. The circle reading is twice the altitude which thereby reduces the precision of the instrument to 12 seconds of arc.

A bubble sextant (bubble octant) [17] contains its own artificial horizon. In measuring altitudes, the image of the celestial body is brought into coincidence with the image of a circular level bubble which forms the artificial horizon. The altitude is then read on a micrometer drum. The fine drum is divided into 2 minute intervals which can be interpolated to the nearest 1 minute. In a bubble sextant such as the Bendix "Pioneer", provision is made to record a series of altitudes automatically. An average reading can be determined from these readings.

These instruments are not capable of first order geodetic accuracy. The positional error can be a maximum of 50 meters from the sextant with the artificial horizon, and 600 meters for the bubble sextant. This, of course, does not take into account, sextant internal errors, bubble errors, and errors in the star tables. In addition, the recording of each measurement using the common sextant will burden the astronauts. With both instruments each star must be identified by the astronauts, leading to further possibilities of error. Time recording must also be done manually.

Using this method (see Figure 1) we can find azimuth from the formula as given by Mueller [16]

$$\sin A = \frac{-\cos d \sin h}{\sin Z}$$

where $h = LHA_{\Omega} - \lambda - \alpha^{\Omega}$

We can find the latitude from the basic formula as given by Mueller [16]

$$\cos Z = \sin d \sin \Phi + \cos d \cos h \cos \Phi$$

and we can determine longitude from the formula as given by Mueller [16]

$$\cos h = \frac{\cos Z - \sin d \sin \Phi}{\cos d \cos \Phi}$$

2.4.2 Method 2: Measurement with the Alignment Optical Telescope

A relative bearing and altitude of a star can be determined by the Alignment Optical Telescope (AOT) which is currently installed in the Lunar Module (LM). An astronomic position on the lunar surface can be established by the use of this instrument in conjunction with the Inertial Measurement Unit (IMU) and the Primary Guidance Navigation System (PGNCS) accelerometers. The great advantage of this method lies in the fact that no additional equipment or training of the astronauts is necessary to obtain an astronomical postion. An apparent disadvantage is the fact that only one astronomical position can be determined during each landing due to the

fact that the equipment is fixed in the lunar module which in turn is fixed on the lunar surface.

The AOT as described in the Grumman manual [4] is a unity power periscope type device with a 60° conical field of view. Its primary purpose is to provide a method of establishing an inertial reference with respect to celestial bodies for inflight and lunar surface operations. It is operated manually by the astronauts and is mounted on the PGNCS navigation base to establish a mechanical alignment and common reference with the IMU. The AOT has a moveable shaft axis which is parallel to the LM "X" axis and a Line of Sight (LOS) axis which is the center of field of view and fixed at 45° from the LM + "X" axis.

The AOT LOS is fixed in elevation and moveable in azimuth to six detent positions. These detent positions are located at 60° and are selected manually by turning a detent selector knob on the AOT. Three of the positions can be used operationally for star sightings and are called forward, left, and right (see Figure 3). The forward, or zero detent position places the LOS in the x,z plane looking forward and up. The right, or +60° position places the LOS 60° to the right of the x,z plane and the left or -60° position places the LOS 60° to the left of the x,z plane. Each of these positions maintain the LOS at 45° from the LM + X axis. The remaining three detent positions are storage positions with the position 180° from the forward position being the normal storage position. The reticle control makes it possible for manual rotation of the reticle for use in lunar surface alignments. The AOT reticle pattern consists of cross hairs and superimposed archimedes spiral (see Figure 4).

The vertical cross hair is an orientation line designated the "Y" line and is parallel to the LM X axis when the reticle is at the 0° reference position. The horizontal cross hair is an auxiliary line designated the "X" line and is perpendicular to the orientation line. A one turn spiral is superimposed from the center of the field of view to the top of the vertical

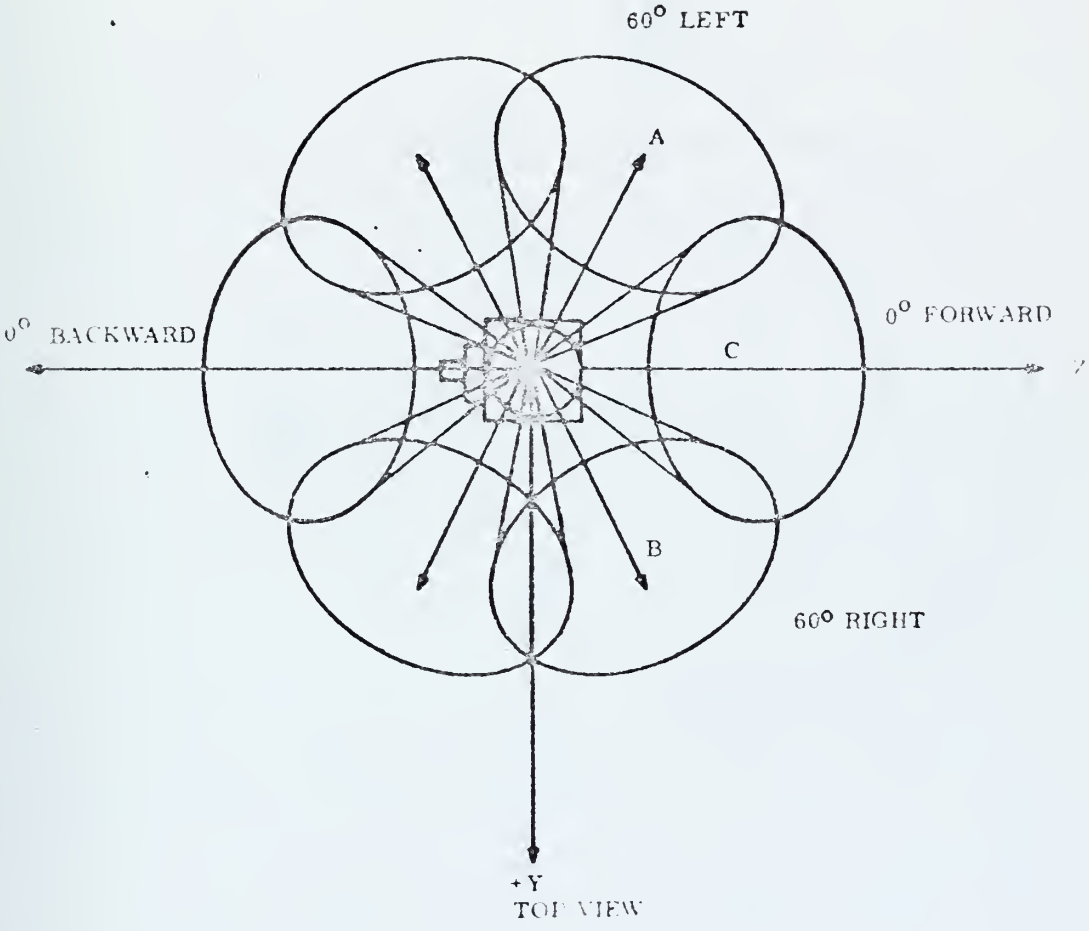

FIGURE 3. - AOT Line of Sight Positions

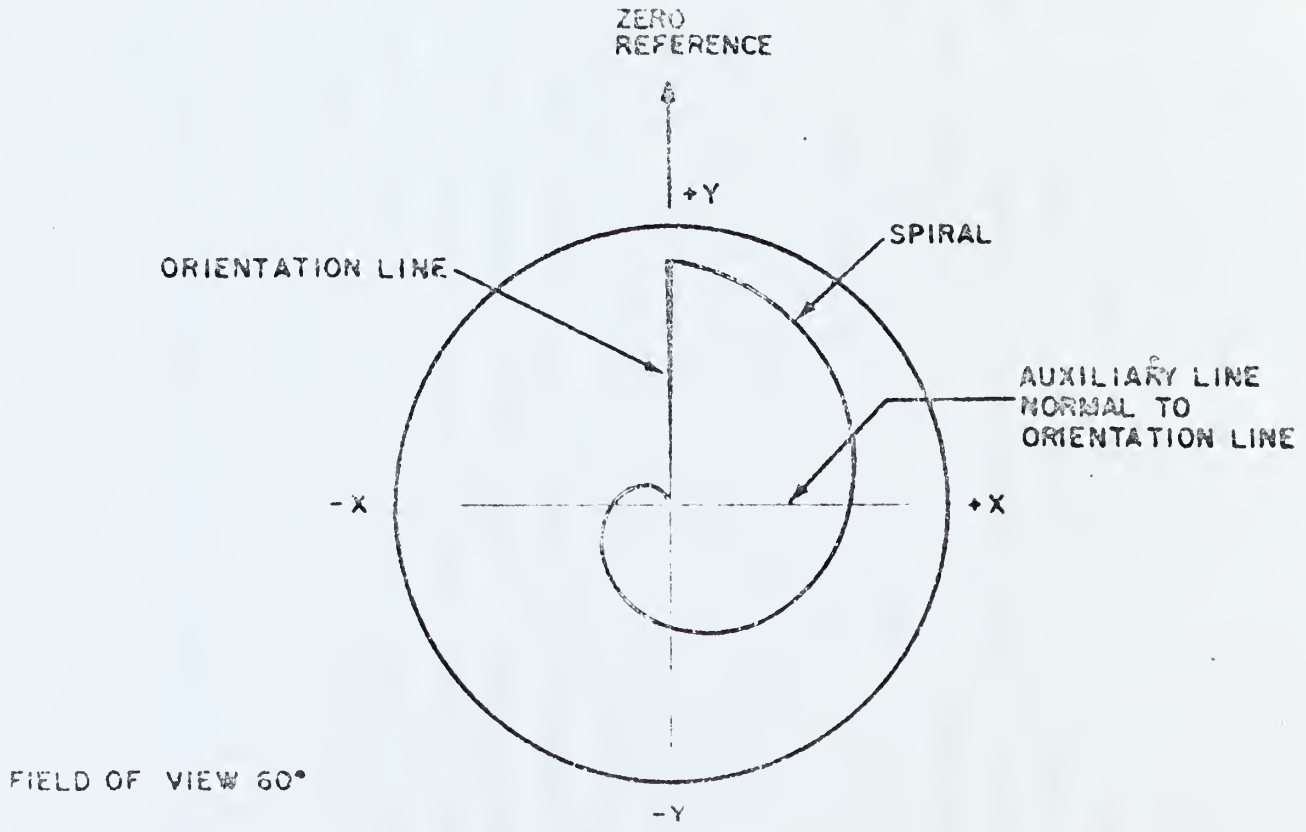

FIGURE 4 . - AOT Reticle Pattern

cross hair. The reticle is edge illuminated.

A counter located on the left side of the AOT, displays an angular readout of reticle rotation. The counter reads in degrees to within ±0.02 degrees or ±72 seconds. Interpolation is possible to within ±0.01 degrees.

On the lunar surface, the selected star can be sighted in either the AOT left, right or forward positions. The astronaut using the manual drive knob, adjusts the reticle to superimpose the orientation line on the target star. This reticle angle displayed on the AOT counter is then manually inserted into the Lunar Module Guidance Computer (LGC) via the Display Console (DSKY). This provides the computer with the star orientation angle (shaft angle). The astronaut then continues to rotate the reticle until a point on the spiral is superimposed on the target star. This second angular readout is then entered into the LGC via the DSKY. The AOT detent position and the star code number are also inserted into the LGC via the DSKY. The LGC can now calculate the angular displacement of the star from the center of the field of view by computing the difference between the two counter readings. Due to the characteristics of the reticle spiral, this Δangle is proportional to the distance of the star from the center of the field of view. Using this Δangle and the proportionality equation, the computer is then able to calculate the trunnion angle. During the lunar surface phase of the lunar landing mission, the Mission Control Center and the LGC use the unit gravity vector as measured by the LM PGNCS accelerometers to align the LM platform and to estimate the latitude and longitude of the LM on the lunar surface.

The AOT star alignment establishes an inertial reference by employing the following formulas:

$$\vec{S}_A = \begin{bmatrix} \vec{S}_1 \\ (\vec{S}_1 \times \vec{S}_2) \times \vec{S}_1 \\ \vec{S}_1 \times \vec{S}_2 \end{bmatrix} \begin{bmatrix} X \\ Y \\ Z \end{bmatrix}_{MCI} = [A]\ [MCI]$$

Where $\vec{S}_1$ and $\vec{S}_2$ are known unit vectors of stars in moon centered inertial space and MCI is the unknown coordinates of the spacecraft with respect to the moon centered inertial system.

$$\vec{S}_B = \begin{bmatrix} \vec{S}_{1M} \\ (\vec{S}_{1M} \times \vec{S}_{2M}) \times \vec{S}_{1M} \\ \vec{S}_{1M} \times \vec{S}_{2M} \end{bmatrix} \begin{bmatrix} X \\ Y \\ Z \end{bmatrix}_{SM} = [B]\ [SM]$$

Where $\vec{S}_{1M}$ and $\vec{S}_{2M}$ are measured unit vectors of stars in stable member space of the stars, and SM is the assumed stable member coordinates referenced to the moon centered inertial coordinate system.

$$[S_A] = [S_B]$$

$$[A]\ [MCI] = [B]\ [SM]$$

$$[SM] = [B]^{-1}\ [A]\ [MCI]$$

$$[\dot{}\,REFSMMAT] = [B]^{-1}\ [A]$$

Therefore: $$MCI = [REFSMMAT]^T\ [SM]$$

Upon comparison with the gravity vector and an estimate of the lunar radius at the point, a position on the lunar surface can then be estimated.

Considering only the precision of the counter reader (with interpolation) we see that the positional accuracy may be as poor as 152 meters or 498 feet. If we considered the errors in the determination of the unit gravity vector, and the errors in the star tables, we would obviously find that this system is not adequate for determining accurate positions on the lunar surface. Considering a minimum standard error of 20".8, we will eliminate this system from consideration for geodetic purposes.

2.4.3 Method 3: Measurement of Relative Azimuth Angles

Method three involves the simultaneous determination of longitude, latitude, and azimuth based on the motion of stars in azimuth. An ordinary theodolite can, of course be used, but it again suffers the drawbacks mentioned in Method 1.

This method though, lends itself to a concept which can allow automatic determination of astronomic position and azimuth. An "Electronic Zenith Camera" (EZC) is currently under development by the Control Data Corporation of Minneapolis, Minnesota. It is described by Carroll as a portable sensor-computer combination which performs both detection of stars and calculation of astronomic position [1] [2]. Stars are detected by their transits across a fan of radial slits placed at the focal surface of a vertically oriented optical system.

The principal advantages of this system is that once set up, the system can determine its astronomical position on the lunar surface without further attention from the astronauts. The system itself can be easily set up on the lunar surface. This set up includes approximate north orientation, and approximate levelling. If necessary, the system could be left to operate after the astronauts have left the lunar surface. Radio transmission of current updated positions could be relayed to earth if necessary.

It is considered that astronomical longitude and latitude can be determined to within 0.3 (1σ) seconds and azimuth to within 3 (1σ) seconds (not considering star catalogue errors) which is certainly acceptable accuracy at this time. No instrument of this type has currently been manufactured, but all advance planning has been completed and the necessary technical skill is available to produce this instrument.

The EZC can be broken down into the system block diagram as seen in Figure 5.

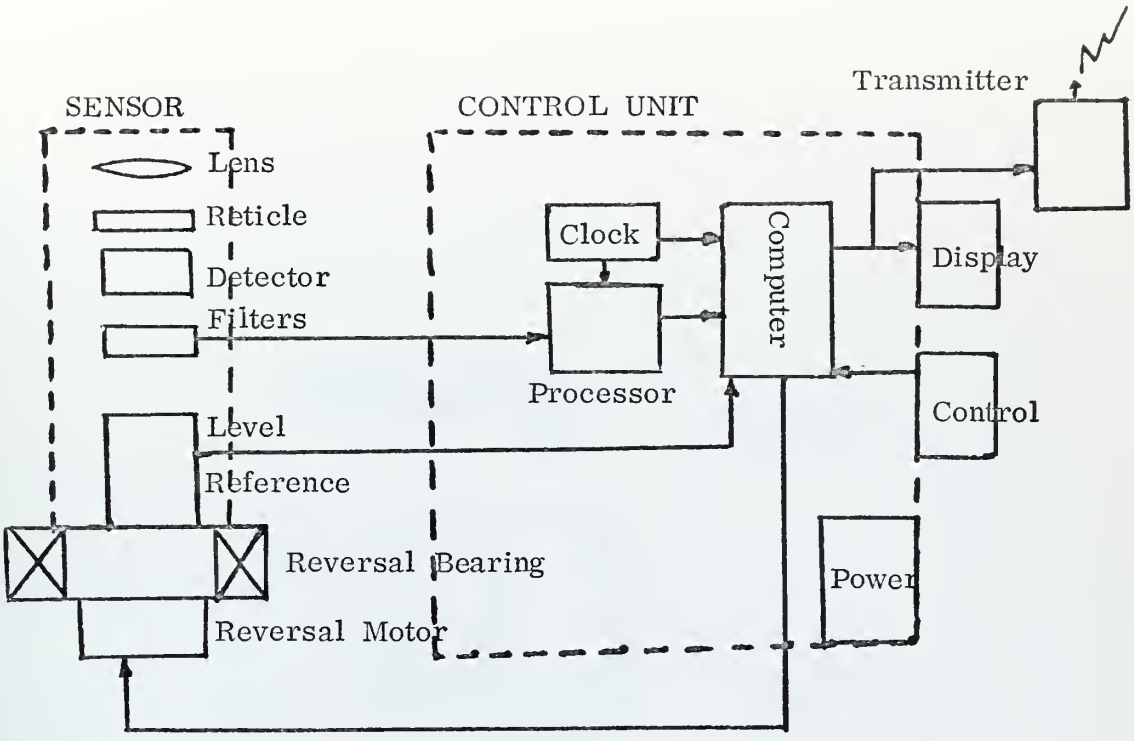

Figure 5. - EZC Block Diagram

We will examine each component starting with the sensor (see Figure 6). The lens system is an f/3.3 system having a 3 centimeter aperture and a 10 centimeter focal length. The lens system has a 16 degree total field of view (eight degrees maximum off-axis angle), and can form an image of a point source restricted to a tangential dimension no greater than 10 seconds of arc but not restricted by the radial dimension. It will be necessary to shield the lens from such bright bodies as the sun and earth.

The reticle has 100 radial slits (at the focal point of the lens) about 1.4 centimeters long and 4.8 microns wide.

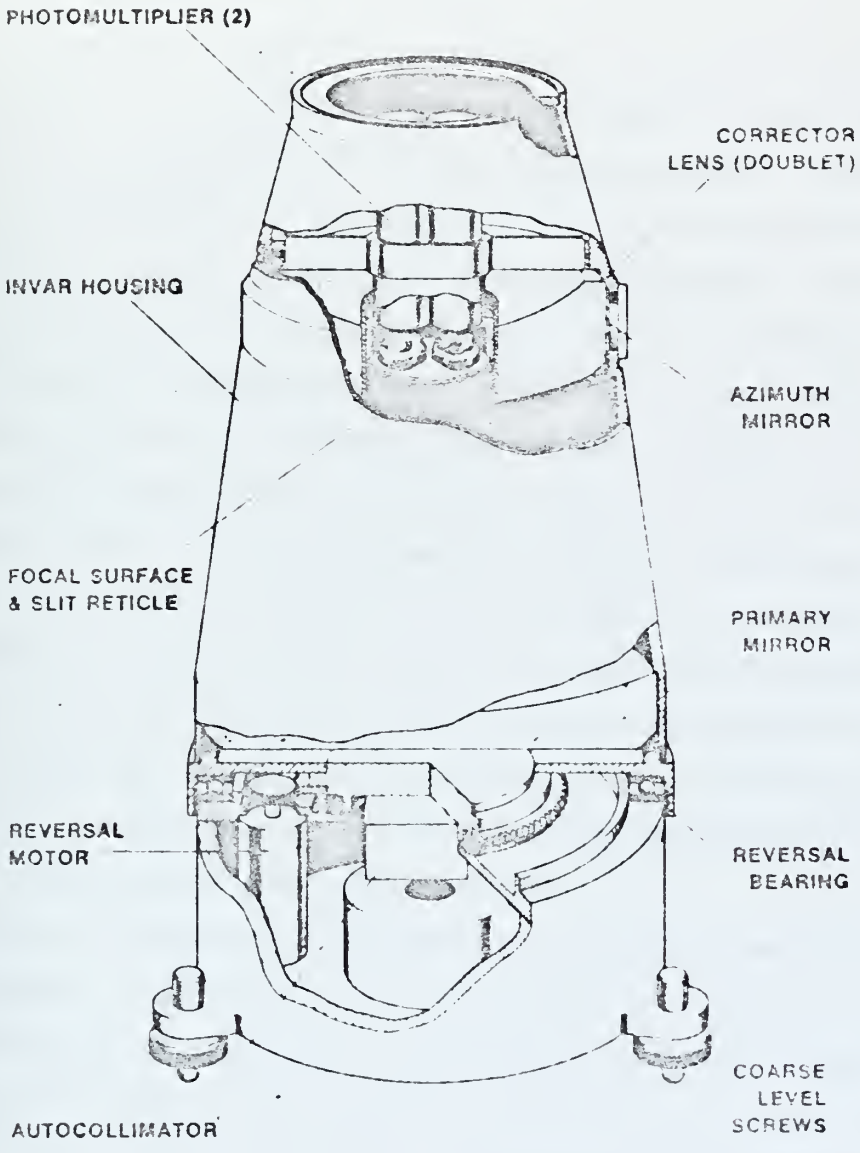

Figure 6. - EZC Sensor Unit

Directly behind the slit reticle is placed an end-window photomultiplier tube which collects all light passing through the slits. The output of this tube is amplified, filtered, and processed so that only the maximum signal (peak pulse) will be recorded and timed. The time input can be any commercially available temperature compensated crystal oscillator.

Looking at the control unit, (see Figure 7) we find that the heart of the system is a miniature general purpose digital computer from which the sensor is controlled, and from which the operator receives status and calculated information. Also included are a precision oscillator (crystal oscillator), a power source, and the necessary interface electronics. The level reference is a mercury pool autocollimator. Miniature electronic autocollimators can reflect a beam off the surface of a completely enclosed mercury pool (dust free surface), the surface of which is covered by a silicone fluid which damps out ripples. If the unit is to function during the lunar night, it will be necessary to heat the mercury pool, due to the lunar temperature being below the freezing point of mercury.

The DC reversal motor is under command of the control unit. The motor drives the instrument about the vertical axis against one of two stops placed 180° apart. The reversal bearing is composed of dissimilar metals (brass and bronze) thereby eliminating the possibility of microscopic welds, which would inhibit accuracy.

Prior to operation, the astronaut must level the instrument to within 30 seconds. Within this range the automatic level reference supplies information to the computer so as to measure the angle between the instrument vertical axis and the true local vertical. The astronaut must also make an initial north (south) - alignment of the instrument. This can be accomplished by using a gunsight mechanism on the equipment and sighting with the aid of near polar stars such as previously described. This will yield an initial approximation of north, with the exact azimuth to be solved for.

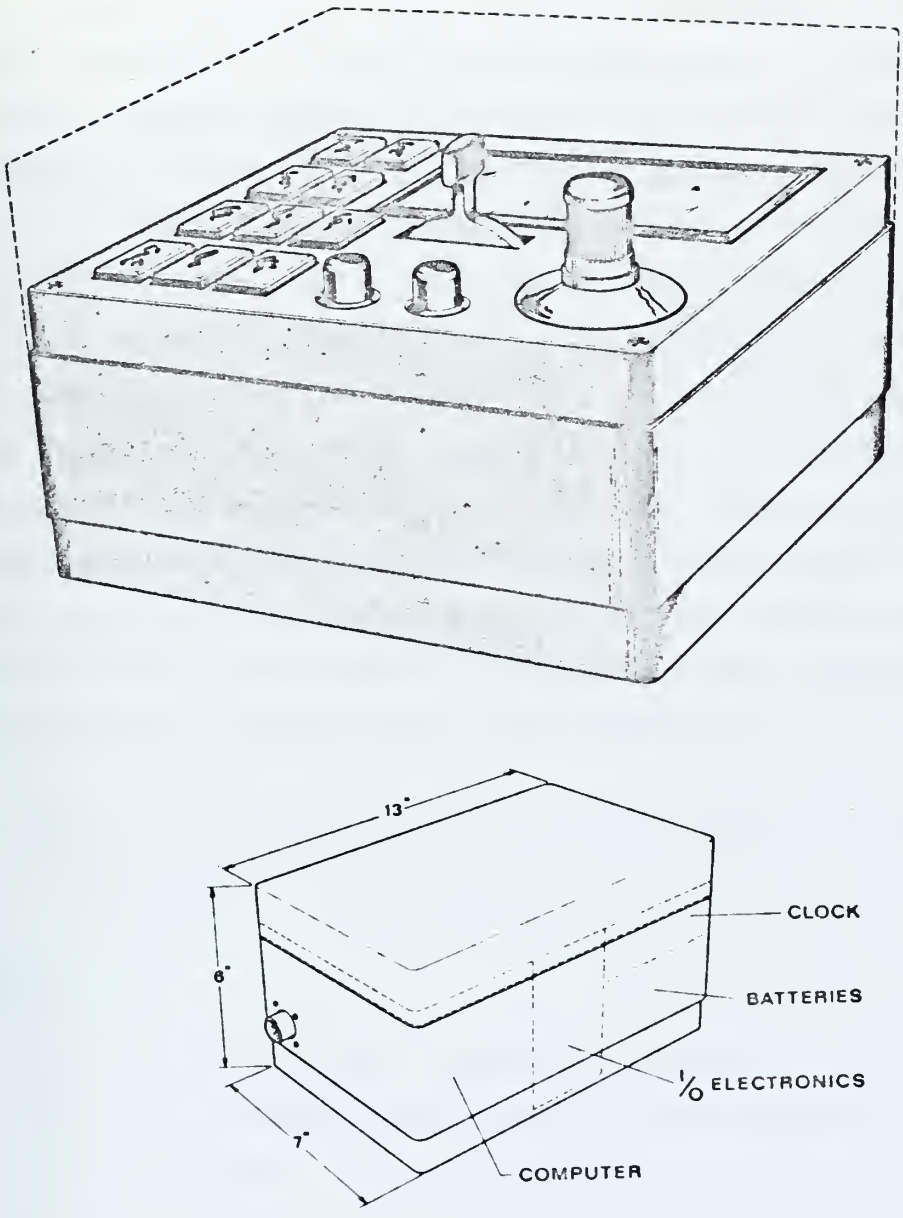

Figure 7. - EZC Control Unit

We are interested in detecting stars from +1. to +5.3 magnitude. It has been determined that the best results are obtained with a star transiting at least one slit each minute. In order to achieve this rate on the lunar surface, we must either wait approximately 27 times longer for a solution than we would on earth (approximately 27 hours) or have an internal spinning reticle which would reduce the solution time but would introduce additional errors into the system (approximately 1-arc second).

Star identification is based on an approximate knowledge of the observer's position, and north alignment. The computer determines the expected pattern of transit times from the stored star catalog. This computed pattern and the measured time pattern are then superimposed, and these target pairs which correspond closely and uniquely in magnitude constitute tentative identifications. These are then used to adjust the assumed position and azimuth and thereby to adjust slightly the computer time pattern so as to obtain a better fit with the measured pattern. From here the final solution sequence preceeds by solving a linearized version of the following equation derived from equations 2.2:

$$\cot(A_o + \beta_j)\sin(LHA_\Omega - \lambda - \alpha_i^\Omega) - \sin\Phi\cos(LHA_\Omega - \lambda - \alpha_i^\Omega) + \tan d_i \cos\Phi = 0$$

where

A_o - The azimuth of the 0th slit (dependent on north alignment)

β_j - The fixed angle between the Jth slit and the 0th slit

LHA_Ω - Apparent lunar reference meridian hour angle of the node (LADT)

λ - Longitude

α_i - Lunar right ascension of the i th star

Φ - Latitude

d_i - Lunar declination of the i th star

This linearized version is then

$$0 = \sin A_j \cot Z \, d\Phi + \cos\Phi(\tan\Phi - \cos A_j \cot Z)\, dh - dA_o$$

where Z is the computed zenith distance

$$h = LHA_\Omega - \lambda - \alpha_i^\Omega$$

$$A_j = A_o + \beta_j$$

and

$$\cot Z = \frac{(\sin d \sin\Phi + \cos d \cos h \cos\Phi) \sin A_j}{-\cos d \sin h}$$

The measured quantities are azimuth and time. Latitude and longitude of the station are assumed.

Since there are more measurements than unknowns, we may use a least square solution, with a Kalman filtering technique [10] based on the Newton-Raphson iteration formula, so that matrix inversions will not be required. This iterative procedure is based on the following equation:

$$X_{N+1} = X_N - C_N a_N' \frac{[a_N X_N + L_N]}{[1 + a_N C_N a_N']}$$

where:

$$\text{matrix } X_N = {}_3X_1 = \begin{bmatrix} d\Phi \\ dh \\ dA_o \end{bmatrix} \qquad X_o = \begin{bmatrix} 0 \\ 0 \\ 0 \end{bmatrix}$$

$$\text{matrix } a_N = {}_1a_3 = (\sin A_j \cot Z_i - \cos\Phi\ (\tan\Phi - \cos A_j \cot Z_i) - 1)$$

$$L_N = \cot(A_o + A_j) \sin(LHA_\Omega - \lambda - \alpha_i^\Omega) - \sin\Phi \cos(LHA_\Omega - \lambda - \alpha_i^\Omega) + \tan d_i \cos\Phi$$

and matrix $C_{N+1} = C_N - \frac{C_N\, a_N'\, a_N\, C_N}{[1 + a_N\, C_N\, a_N']}$

where matrix $C_o = {}_3C_3 = (\bar{A}'\,\bar{A})^{-1}$

where the rows of $\bar{A}$ are the rows of a_1 to a_5.

We can see that the incorporation of a new measurement does not require a new matrix inversion. Only one inversion is required and that is for C_o which is only an inversion of a 3 x 3 matrix. After the first five marks no old observation information need be saved. The values of the elements of matrix C are indicative of the quality of the results. Matrix C is the covariance matrix, but only under the assumption that there are no systematic errors in the residual vector L. There are systematic errors in the residual vector L, due to the timing error (τ libration) and the errors in star right ascension and declinations. In order to cancel alignment errors in the optical-reticle system and normality errors between the instrument axis, the instrument is rotated 180°, and the astronomic position is again determined. The average of these positions is then used. The level status of the reversal bearing is also measured and it is applied as a final correction.

2.4.4 Method 4: Measurement with Photography

The determination of astronomical position by photography can be accomplished with a photo-theodolite or other metric camera using methods such as one or three. The drawbacks of a photo-theodolite are the same as for an ordinary theodolite and thus would tend to make it impractical for early missions.

As described in the Geonautics study [7], a metric camera could be used as a zenith camera or otherwise fixed in elevation to photograph stars.

Various sophisticated systems such as gravity-operated automatic leveling devices with gimballed camera support, electronically operated automatic leveling devices, gyroscopic devices, etc., could be considered to level the camera. The simplest and most feasible device would seem to be the conventional spirit bubbles. These bubbles could be placed on a camera support such as a tripod, so that the camera, when placed on the support, could be theoretically leveled within the range of two orthogonally placed precise level vials inside the camera body. These precise levels can be photographed during each exposure, thus providing a permanent record of the level reference. Drawbacks in this system tend to lie in the fact that the bubbles are affected by differential heating from external light, so that they must be protected both from radiant heat and from light. The bubble, of the sensitivity required in the camera, would be termed a "slow" bubble in a conventional surveying instrument. It would be even slower on the lunar surface due to the moon's smaller gravitational force.

This method provides a permanent and true record of field data as film can be removed from camera and returned to earth. Most advantageous is the fact that a great number of measurements can be taken in a minimum amount of time after the initial set up. There is a requirement for extra equipment such as a tripod, but it could be retractable and made of aluminum or some similar material Timing of each photo would also be required, but this could be done by an internal clock, which would furnish the time to be included in the edge data.

2.5 Error Analysis

Let us first consider the errors which contribute to the lunar apparent selenoequatorial coordinates. In the transformation of the mean geoequatorial coordinates to the mean ecliptic coordinates, the relatively small errors in α , δ , and ϵ can be considered negligible. Therefore, β and λ can be considered errorless. In the transformation of the mean ecliptic coordinates

to the mean selenoequatorial coordinates we consider that the error in Ω is negligible, but there is definitely an error in inclination (I). Let us make a conservative estimate of 20" for this error. Differentiating equations (2.1) we see that the results are similar to that given by Mueller [16].

$$dd_m = \cos\alpha_m^{\Omega} \sin I \, d(\lambda - \Omega) + (\sec d_m \sec\beta \cos I - \tan d_m \tan\beta) \, d\beta + \sin\alpha_m^{\Omega} \, dI$$

but $d(\lambda - \Omega) = 0$

$d\beta = 0$

therefore $dd_m = \sin\alpha_m^{\Omega} \, dI$ and therefore the maximum value of

$$dd_m = \sin\alpha_m^{\Omega} \, dI = 20''.0 \sin\alpha_m^{\Omega}$$

and $$d\alpha_m^{\Omega} = (\sec^2 d_m \cos I - \sec d_m \tan d_m \sin\beta) \, d(\lambda - \Omega) - \cos\alpha_m^{\Omega} \sec\beta \sec d_m \sin I \, d\beta - \tan d_m \cos\alpha_m^{\Omega} \, dI$$

but again $d(\lambda - \Omega) = 0$

$d\beta = 0$

therefore $d\alpha_m^{\Omega} = -\tan d_m \cos\alpha_m^{\Omega} \, dI = -20''.0 \tan d_m \cos_m^{\Omega}$

Considering the transformation of mean into apparent selenoequatorial coordinates, we will use the following equations:

$$\begin{aligned} d\alpha_{sapp}^{\Omega} = {} & d\alpha_m^{\Omega} + \frac{\partial A_1 a_1}{\partial \sigma} d\sigma + \frac{\partial A_1 a_1}{\partial I} dI + \frac{\partial A_1 a_1}{\partial d_m} dd_m \\ & + \frac{\partial A_1 a_1}{\partial \alpha_m^{\Omega}} d\alpha_m^{\Omega} + \frac{\partial B_1 b_1}{\partial \rho} d\rho + \frac{\partial B_1 b_1}{\partial I} dI + \frac{\partial B_1 b_1}{\partial d_m} dd_m \\ & + \frac{\partial B_1 b_1}{\partial \alpha_m^{\Omega}} d\alpha_m^{\Omega} + \frac{\partial C_1 c_1}{\partial \alpha_m^{\Omega}} d\alpha_m^{\Omega} + \frac{\partial C_1 c_1}{\partial I} dI + \frac{\partial C_1 c_1}{\partial d_m} dd_m \\ & + \frac{\partial D_1 d_1}{\partial \alpha_m^{\Omega}} d\alpha_m^{\Omega} + \frac{\partial D_1 d_1}{\partial I} dI + \frac{\partial D_1 d_1}{\partial d_m} dd_m \end{aligned} \qquad (2.3)$$

and a similar expression for dd_{sapp}, considering in both cases a negligible error in proper motion.

In the following differential expressions we will assume:

$\cos I = 1$

d_m = Limited to 45°

$\rho = 1'$

$\sigma = 1'$

The differential quantities will be assigned the following conservative values:

$d\sigma$	=	10"	=	.000050 radians	(estimate from [13])
$d\rho$	=	10"	=	.000050 radians	(estimate from [13])
dI	=	20"	=	.000097 radians	
dd_m	=	20"	=	.000097 radians	
$d\tau$	=	15"	=	.000014 radians	(estimate)
$d\alpha^{\Omega}_{m}$	=	20"	=	.000097 radians	

$$A_1 a_1 = (P^d_o t + \sigma)(\cos I - \sin I \sin\alpha^{\Omega}_{m} \tan d_m)$$

$$\frac{\partial A_1 a_1}{\partial \sigma} d\sigma = (\cos I - \sin I \sin\alpha^{\Omega}_{m} \tan d_m)\, d\sigma$$
$$= (1 - .02676 \sin\alpha^{\Omega}_{m} \tan d_m)\, d\sigma = d\sigma$$
$$= 10".0$$

$$\frac{\partial A_1 a_1}{\partial I} dI = (P^d_o t + \sigma)(\cos I \sin\alpha^{\Omega}_{m} \tan d_m - \sin I)\, dI$$
$$= (-.0015059)(-.97324)\, dI$$
$$= 0".0$$

$$\frac{\partial A_1 a_1}{\partial d_m} dd_m = (P^d_o t + \sigma)(\sin I \sin\alpha^{\Omega}_{m} \sec^2 d_m)\, dd_m$$
$$= (-.0015059)(.05352)\, dd_m$$
$$= 0".0$$

$$\frac{\partial A_1 a_1}{\partial \alpha_m^{\Omega}} d\alpha_m^{\Omega} = (P_o^d t + \sigma)(-\sin I \cos \alpha_m^{\Omega} \tan d_m) d\alpha_m^{\Omega}$$

$$= (-.0015059)(-.02676)\, d\alpha_m^{\Omega}$$

$$= 0''.0$$

$$B_1 b_1 = \rho \cos \alpha_m^{\Omega} \tan d_m$$

$$\frac{\partial B_1 b_1}{\partial \rho} d\rho = \cos \alpha_m^{\Omega} \tan d_m \, d\rho$$

$$= 10''.0 \cos \alpha_m^{\Omega} \tan d_m$$

$$\frac{\partial B_1 b_1}{\partial I} dI = 0''.0$$

$$\frac{\partial B_1 b_1}{\partial d_m} dd_m = \rho \cos \alpha_m^{\Omega} \sec^2 d_m \, dd_m$$

$$= .00058\, dd_m$$

$$= 0''.0$$

$$\frac{\partial B_1 b_1}{\partial \alpha_m^{\Omega}} d\alpha_m^{\Omega} = \rho \sin \alpha_m^{\Omega} \tan d_m \, d\alpha_m^{\Omega}$$

$$= -(.00029)\, d\alpha_m^{\Omega}$$

$$= 0''.0$$

$$C_1 c_1 = K \sin(L_{ap} - \Omega + 180^\circ) \cos I \cos \alpha_m^{\Omega} \sec d_m \, dI$$

$$\frac{\partial C_1 c_1}{\partial I} dI = -K \sin(L_{ap} - \Omega + 180^\circ) \sin I \cos \alpha_m^{\Omega} \sec d_m \, dI$$

$$= (.000097)(1)(.02676)(1)(1.4)\, dI$$

$$= 0''.0$$

$$\frac{\partial C_1 c_1}{\partial d_m} dd_m = K \sin(L_{ap} - \Omega + 180^\circ) \cos I \tan d_m \sec d_m \cos \alpha_m^{\Omega} \, dd_m$$

$$= (.000097)(1)(.02676)(1)(1)(1.4)\, dI$$

$$= 0''.0$$

$$\frac{\partial C_1 c_1}{\partial \alpha_m^{\Omega}} d\alpha_m^{\Omega} = -K \sin(L_{ap} - \Omega + 180^\circ) C = SI \sin \alpha_m^{\Omega} \sec d_m \, d\alpha_m^{\Omega}$$
$$= (.00097)\ (1)\ (.02676)\ (1)\ (1.4)\, d\alpha_m^{\Omega}$$
$$= 0''.0$$

$$D_1 d_1 = K \cos(L_{ap} - \Omega + 180^\circ) \sin \alpha_m^{\Omega} \sec d_m$$

$$\frac{\partial D_1 d_1}{\partial I} dI = 0''.0$$

$$\frac{\partial D_1 d_1}{\partial d_m} dd_m = K \cos(L_{ap} - \Omega + 180^\circ) \sin \alpha_m^{\Omega} \tan d_m \sec d_m \, dd_m$$
$$= (.000097)\ (1)\ (1)\ (1)\ (1.4)\, dd_m$$
$$= 0''.0$$

$$\frac{\partial D_1 d_1}{\partial \alpha_m^{\Omega}} d\alpha_m^{\Omega} = K \sin(L_{ap} - \Omega + 180^\circ) \cos \alpha_m^{\Omega} \sec d_m \, d\alpha_m^{\Omega}$$
$$= (.000097)\ (1)\, d\alpha_m^{\Omega}$$
$$= 0''.0$$

We will now consider the standard error in lunar right ascension. We will use the quadratic form of equation 2.3, eliminating terms which are zero. We will assume that $d\alpha_m^{\Omega}$ and

$$\frac{\partial B_1 b_1}{\partial \rho} d\rho$$

are dependent terms while all other non-zero terms are independent. Therefore,

$$(d\alpha_{sapp}^{\Omega})^2 = (d\alpha_m^{\Omega})^2 + \left(\frac{\partial A_1 a_1}{\partial \sigma} d\sigma\right)^2 + \left(\frac{\partial B_1 b_1}{\partial \rho} d\rho\right)^2 + \frac{\partial B_1 b_1}{\partial \rho} d\alpha_m^{\Omega} d\rho$$

$$= 400 \tan^2 d_m \cos^2 \alpha_m^{\Omega} + 100 + 100 \tan^2 d_m \cos^2 \alpha_m^{\Omega} - 200 \tan^2 d_m \cos^2 \alpha_m^{\Omega}$$

and $$d\alpha_{sapp}^{\Omega} = \sqrt{300 \tan^2 d_m \cos^2 \alpha_m^{\Omega} + 100}$$

$$A_1 a_1' = +(P_o^d t + \sigma) \sin I \cos \alpha_m^{\Omega}$$

$$\frac{\partial A_1 a_1'}{\partial \sigma} d\sigma = \sin I \cos \alpha_m^{\Omega} d\sigma$$

$$= .02676 \cos \alpha_m^{\Omega} d\sigma$$

Max. value = 0".5 (will be neglected)

$$\frac{\partial A_1 a_1'}{\partial I} dI = (P_o^d t + \sigma) \cos I \cos \alpha_m^{\Omega} dI$$

$$= -.0015059\, dI$$

$$= 0".0$$

$$\frac{\partial A_1 a_1'}{\partial d_m} dd_m = 0".0$$

$$\frac{\partial A_1 a_1'}{\partial \alpha_m^{\Omega}} d\alpha_m^{\Omega} = -(P_o^d t + \sigma) - \sin I \sin \alpha_m^{\Omega} d\alpha_m^{\Omega}$$

$$= (-.0015059)\ (-.02676)\ (1)\ (d\alpha_m^{\Omega})$$

$$B_1 b_1' = \rho \sin \alpha_m^{\Omega}$$

$$\frac{-\partial B_1 b_1'}{d\rho} d\rho = -\sin \alpha_m^{\Omega} d\rho$$

$$\frac{\partial B_1 b_1'}{\partial I} dI = 0".0$$

$$\frac{\partial B_1 b_1'}{d_m} dd_m = 0".0$$

$$\frac{\partial B_1 b_1'}{\partial \alpha_m^{\Omega}} d\alpha_m^{\Omega} = \rho \cos \alpha_m^{\Omega} d\alpha_m^{\Omega}$$

$$= -.00029\, d\alpha_m^{\Omega}$$

$$= 0".0$$

$$C_1 c_1' = -K \sin (L_{ap} - \Omega + 180^\circ) \cos I \sin \alpha_m^{\Omega} \sin d_m$$

$$-K \sin (L_{ap} - \Omega + 180^\circ) \sin I \cos d_m$$

$$\frac{\partial C_1 c_1'}{\partial I} dI = (+ K \sin(L_{ap} - \Omega + 180^\circ) \sin I \sin\alpha_m^\Omega \sin d_m - K \sin(L_{ap} - \Omega + 180^\circ) \cos I \cos d_m) dI$$

$$= -.00007\ dI$$

$$= 0''.0$$

$$\frac{\partial C_1 c_1'}{\partial d_m} dd_m = (- K \sin(L_{ap} - \Omega + 180^\circ) \cos I \sin\alpha_m^\Omega \cos d_m + K \sin(L_{ap} - \Omega + 180^\circ) \sin I \sin d_m) dd_m$$

$$= -.00007\ dd_m$$

$$= 0''.0$$

$$\frac{\partial C_1 c_1'}{\partial \alpha_m^\Omega} d\alpha_m^\Omega = - K \sin(L_{ap} - \Omega + 180^\circ) \cos I \cos\alpha_m^\Omega \sin d_m$$

$$= .00007\ d\alpha_m^\Omega$$

$$= 0''.0$$

$$D_1 d_1' = - K \cos(L_{ap} - \Omega + 180^\circ) \cos\alpha_m^\Omega \sin d_m$$

$$\frac{\partial D_1 d_1'}{\partial I} dI = 0''.0$$

$$\frac{\partial D_1 d_1'}{\partial d_m} dd_m = - K \cos(L_{ap} - \Omega + 180^\circ) \cos\alpha_m^\Omega \cos d_m$$

$$= .00007\ dd_m$$

$$= 0''.0$$

$$\frac{\partial D_1 d_1'}{\partial \alpha_m^\Omega} d\alpha_m^\Omega = K \cos(L_{ap} - \Omega + 180^\circ) \sin\alpha_m^\Omega \sin d_m$$

$$= .00007\ d\alpha_m^\Omega$$

$$= 0''.0$$

We will now consider the standard error in lunar declination. We will use the quadratic form of the similar declination equation 2.3, eliminating terms which are zero. We will assume dd_m and

$$\frac{\partial B_1 b_1' d\rho}{\partial \rho}$$

are dependent terms.

Therefore,

$$(dd_{sapp})^2 = (dd_m)^2 + \left(\frac{\partial B_1 b_1'}{\partial \rho} d\rho\right)^2 + \frac{\partial B_1 b_1'}{\partial \rho} d\rho\, dd_m$$

$$= 400 \sin^2 \alpha_m^{\Omega} + 100 \sin^2 \alpha_m^{\Omega} - 200 \sin^2 \alpha_m^{\Omega}$$

$$= 300 \sin^2 \alpha_m^{\Omega}$$

and $$dd_{sapp} = 17''.3 \sin \alpha_m^{\Omega}$$

Thus, we can see that if stars with near zero declination are used, we can effectively limit the error in lunar right ascension. Let us examine the circumstances if we use stars with $\pm 10^\circ$ declination and $\pm 10^\circ$ right ascension. The maximum error will then be:

$$d\alpha_{sapp}^{\Omega} = \sqrt{300\ (.03109)\ (1) + 100} = 10''5$$

$$dd_{sapp} = 17''.3\ (.17633) = 3''.1$$

Thus, we can see that there can be an optimum time for which to obtain a position. If we consider limiting α_m^{Ω} to values of 350° right to 010° and 170° right to 190°, we will immediately limit the error in declination to a maximum value of 3".1. See Appendix E for stars which fall into this area.

Next we will consider errors in time. We have defined

$$\text{LMDT} + \text{eq.N} = \text{LADT}$$

or

$$\text{RMDT} + \text{eq.N} = \text{RADT}$$

We can consider that RMDT is errorless so that the error then occurs only in eq.N which is dependent upon σ and τ. So that we may say

$$dT^2 = d\sigma^2 + d\tau^2 + d\sigma\, d\tau$$

or $dT = 10^s.0$ draconic time or $5''.0$ of arc.

We will now consider the standard error of each method in determination of astronomic position.

For Method 1, we will first present the differential formula for latitude [16] :

$$d\Phi = -\sec A\, dZ - \cos\Phi \tan A\, dh - \frac{\sin\Phi \operatorname{cosec} Z \sec d - \tan d \cot Z}{\cos A}\, dd$$

We desire the azimuth to be near 0 or 180 degrees so that

$$d\Phi = -dZ - (\sin\Phi \operatorname{cosec} Z \sec d - \tan d \cot Z)\, dd$$

and if Z equals approximately 45°, then for a station at or near the equator d will also equal about 45° so that

$$d\Phi = -dZ - dd$$

Therefore, for Method 1, these errors are independent, letting $dZ = 7''.0$, and considering

$$(d\Phi)^2 = (7''.0)^2 + (17''.3 \sin\alpha_{\odot}^{\Omega})^2$$

and $$d\Phi = 7''.0 \text{ to } 18''.7$$

Thus, an error in h will have little effect on latitude determination. The error in latitude determination is basically related to the approximate right

ascension. The differential for azimuth [16] is

$$dA = (\sin\Phi\operatorname{cosec}^2 Z - \sin d \operatorname{cosec} Z \cot Z)\, dh + \cos\Phi \sin h \operatorname{cosec}^2 Z\, dd + \cot Z \sin A\, d\Phi$$

If we consider the zenith distance near 90° we see

$$dA = (\sin\Phi - \sin d)\, dh + \cos\Phi \sin h\, dd$$

If the station is near the equator, Φ will be close to 0. Therefore,

$$dA = -\sin d\, dh + \sin h\, dd$$

Finally, we will select a pair of stars close to the meridian, preferably one with 90° north declination and one 90° south. Therefore, $dA = 0$ for stations near the equator when we combine the pair. If we use only a sextant, we will have no means of accurately turning the angle between a star and landmark so that no permanent azimuth could be computed.

The equation for longitude [16] is

$$\lambda = \overset{\Omega}{\alpha}_{sapp} + h - (T + \Delta T_n)$$

where $\overset{\Omega}{\alpha}_{sapp}$ - the apparent right ascension

h - the hour angle as determined

T - the local time on time keeper

ΔT_n - the chronometer correction

Therefore $d\lambda = d\overset{\Omega}{\alpha}_{sapp} + dh - dT_n - d\Delta T_n$

and $$dh = -(\operatorname{cosec} A \sec\Phi dZ + \cot A \sec\Phi\, d\Phi) - \frac{(\tan\Phi \operatorname{cosec} Z \sec d - \tan d \cot Z \sec d)}{\sin A}\, dd$$

The error in h may be eliminated by observing at an azimuth of 90° or 270° and by observing east and west stars in pairs which are symmetrical to the meridian and at the same altitude. Considering $\tan\Phi$ is zero, the star pairs will eliminate the declination errors and zenith error terms.

So that $$d\lambda = d\alpha^{\Omega}_{sapp} - dT - d\Delta T_n$$

$d\Delta T_n$ has little effect on the moon for any ordinary chronometer, so that

$$d\lambda = d\alpha^{\Omega}_{sapp} - dT$$

Therefore $$d\lambda^2 = (d\alpha^{\Omega}_{sapp})^2 + (dT)^2 - dT\, d\alpha^{\Omega}_{sapp}$$

$$= 300 \tan^2 d_m \cos^2 \alpha^{\Omega}_{m} + 100 + 25.0 -$$

$$5. \sqrt{300 \tan^2 d_m \cos^2 \alpha^{\Omega}_{m} + 100}$$

Limiting d_m to 45°, we see

$$d\lambda = 8''.6 \text{ to } 18''.0$$

For Method 2, we have already stated that the low precision of the AOT precludes further consideration.

For Method 3, with impersonal operation and high equipment precision, we can consider that the only errors presented will be systematic in nature, and these specifically will be the systematic errors in star coordinates and time. Thus, we can consider that an astronomic position by the use of this method will yield errors near the equator (declination $< 10^\circ$)

$$d\Phi = dd_{sapp} = 3''.1 \text{ (for optimum time)}$$

$$d\lambda = d\alpha^{\Omega}_{sapp} - dT$$

$$d\lambda^2 = (d\alpha^{\Omega}_{sapp})^2 + (dT)^2 - dT\, d\alpha^{\Omega}_{sapp}$$

$$d\lambda = 9''.1$$

and $$dA = \sin A_j \cot Z\, d\Phi + \cos\Phi (\tan\Phi - \cos A_j \cot Z)\, d\lambda$$

near the equator, we say

$$dA = (\sin A_j\, d\Phi - \cos A_j\, d\lambda) \cot Z$$

The largest Z we can hope for is 8°, and assigning an azimuth of the j^{th} slit to be 45°, we find:

$$dA^2 = 25\, d\Phi^2 + 25\, d\lambda^2 \quad \text{(considering no dependence)}$$

Therefore, $dA > 50''.0$

For Method 4, the errors are basically the same as for Method 1, if a panoramic camera is used, and basically the same as for Method 3, if the zenith camera is used (considering camera operating at optimum time). See Table 3 for comparison of results.

Method	$d\Phi$	$d\lambda$	dA
1	7".0 - 18".7	8".6 - 18".0	not directly obtainable
2	> 20".8	> 20".8	not directly obtainable
3	3".1 (optimum time)	9".1	> 50".0
4*	3".1 - 18".7	8".6 - 18".0	> 0".0

*Dependent upon horizon or zenith camera type, not including instrument or observation errors.

Table 3. - Estimated Standard Errors (Station Near the Equator)

2.6 Conclusions

Due to the possibility of limiting the error in star coordinates, it would seem that an automatic instrument as described in Method 3, would be the one which would be able to take best advantage of this point. Missions, of course cannot be scheduled so that these star coordinates could be utilized. It would be only coincidence if the current short duration landings occured at the proper time. Thus, the advantages of an instrument which could determine position automatically after the

astronauts depart is apparent. During future missions, if the landings are near the lunar equator, it would seem that the Electronic Zenith Camera/ Zenith photography would take best advantage of the stars with near zero declination. If landing were far removed from the equator, optimum times would need to be recomputed due to the increased error in lunar right ascension, which would result from the higher star declinations. The format of the current missions, therefore, dictates that we use an automatic instrument which could take advantage of stars which offer minimum coordinate errors. The ease of set up and minimum training required for the astronauts, combined with the inherent accuracy of the system, show that the Electronic Zenith Camera or similar instrument is the best possible choice of equipment for the current missions. An accurate azimuth can only be determined by the use of an horizon camera at this time.

It must again be stated that the Electronic Zenith Camera has not yet been manufactured, and could not be included in immediate missions.

3. DEFLECTION OF THE VERTICAL

Deflections of the vertical relating the normals of the astronomic and selenographic systems can be obtained by:

(1) Direct astronomical measurement of latitude and longitude with subsequent comparison with the selenodetic coordinates extended from a datum by triangulation or traverse. The results are affected by accumulation of error in the triangulation or traverse.

(2) Integrating gravity anomalies over large areas surrounding the point where the deflection is required.

(3) Computing the deflections of the vertical due to topography, and then refining this system using some model of isostatic compensation.

(4) Computing the deflections of the vertical from known spherical harmonics.

The first method depends on an assigned deflection at a datum, thus is of no use in this paper. The second method requires gravity anomalies over large areas, and these of course are not available except by obtaining them through method four. But, method four is of little value in deflection computations as the harmonics reflect moon-wide rather than local distribution. The computation of deflections of the vertical requires more local data near the station. Thus, we will investigate method three, but will use method four as a check on the magnitude of the deflections.

In addition, the effect of other bodies on the deflection of the vertical will be calculated.

3.1 Computation of Topographic Deflections of the Vertical

Following the method of Jordan-Eggert [11] adapted for the moon, we consider the influence of the visible masses in the neighborhood of a station.

For this, we imagine the terrain around the station divided into compartments by means of concentric circles and radial lines, so that we obtain a great number of vertical columns between a given reference surface and the moon's physical surface.

If the components of this deflection in the meridian and the prime vertical are expressed by $\Delta\xi$ and $\Delta\eta$ respectively, then we have

$$\Delta\xi = \frac{3\Theta H\rho''}{4\Theta\pi_m a}(\sin\alpha_2 - \sin\alpha_1)\log_e r_2/r_1$$

$$\Delta\eta = \frac{-3\Theta H\rho''}{4\Theta\pi_m a}(\cos\alpha_2 - \cos\alpha_1)\log_e r_2/r_1$$

where Θ_m - The surface layer density

Θ - The mean density of the moon

H - Height above reference surface

a - The radius of the moon

$\alpha_1\ \alpha_2$ - The compartment azimuths

r_1, r_2 - The outer and inner radius of compartments

The reference surface which will be used is defined as a moon centered sphere of radius 1,737.988 kilometers.

We will use the following values for the constants as given in [6].

Θ = 2.670 gm/cm^3 (assumed)*

Θ_m = 3.343 gm/cm^3

a = 1,737,988 meters

ρ = 206,265"

* This figure was obtained from averaging figures in various sources for a surface layer of 10KM. An error in this figure will produce a proportional error in the deflections.

and we obtain

$$\Delta\xi = 0''.0226\ H(\sin\alpha_2 - \sin\alpha_1)\log_e r_2/r_1$$
$$\Delta\eta = 0''.0226\ H(\cos\alpha_2 - \cos\alpha_1)\log_e r_2/r_1$$

Note: H in meters

These two values are to be computed for each terrain section around the point 0, and then the two components of the deflection of the vertical for the point 0 are equal to the algebraic sum of all values of $\Delta\xi$ or of $\Delta\eta$ as:

$$\xi = \sum_{i=1}^{n} \Delta\xi_i \qquad \eta = \sum_{i=1}^{n} \Delta\eta_i$$

We have so far assumed that the whole of the attracting stratum is in the horizon of the station, which for the moon would be grossly in error when only a short distance from the station. Therefore, it is necessary in order to secure the required degree of accuracy to take into account the curvature of the moon's surface. The effect of this curvature is to throw the compartment surface below the horizon of the station. Therefore, when significant, we will use the equation developed by A. R. Clarke, given in [11].

$$\Delta\xi = 0''.0226\ H(\sin\alpha_2 - \sin\alpha_1)\log_e \frac{\tan 1/4\ \Theta_2}{\tan 1/4\ \Theta_1} + \cos 1/2\ \Theta_2 = \cos 1/2\ \Theta_1$$

$$\Delta\eta = -0''.0226\ H(\cos\alpha_2 - \cos\alpha_1)\log_e \frac{\tan 1/4\ \Theta_2}{\tan 1/4\ \Theta_1} + \cos 1/2\ \Theta_2 - \cos 1/2\ \Theta_1$$

in which Θ_2 is r_2 reduced to an arc

$$\Theta_2 = \frac{r_2 \text{ (in km)}}{1{,}737.988} \text{ radians}$$

and Θ_1 is r_1 reduced to an arc

$$\Theta_1 = \frac{r_1 \text{ (in km)}}{1{,}737.988} \text{ radians}$$

Any values for either the constant r_2 / r_1 or for the constant difference $(\sin\alpha_2 - \sin\alpha_1)$ may be adopted arbitrarily. Advantage is taken of this fact to adopt such values as would make the computation as simple and rapid as possible. The values $r_2 / r_1 = 1.19362053$ and $(\sin\alpha_2 - \sin\alpha_1) = 0.25$ were adopted. With these values, the deflection equations will be:

$\Delta\xi$ = .001" h (in meters)

$\Delta\eta$ = .001" h (in meters) (the reference line is shifted 90°)

As a result then, of this particular selection of arbitrary constants defining the limits of the compartments, the deflection produced at the station by the material lying above the reference surface in any compartment is expressed as one second of arc for each kilometer the mean elevation is above the reference surface.

The arbitrary selection of the adopted values of $(\sin\alpha_2 - \sin\alpha_1)$ and r_2, r_1 was guided by three considerations. First, it was important to be as rapid as possible in determining the contribution of each section. The compartments must be small enough to bring the accuracy of the method within required limits and yet large enough to avoid excessive amounts of detail in the computation. The compartments should be compact areas, not long and narrow, in order to facilitate the estimation of the mean elevation within each compartment.

The radii of the adopted circles separating the compartments are shown in Table 4. Each group of sixteen compartments (four in each quadrant) forms a ring. The rings, for convenience of designation,

were assigned serial numbers commencing with the inner ring, (see Figure 8).

It was determined that the curvature of the moon had to be taken into account at ring 46. The outer radii of all succeeding rings were computed iteratively on the IBM 360-75 computer, (see Appendix A).

It was found by Hayford [8], that on the earth, the computed topographic deflections are much larger than the actual deflections of the vertical, in that an influence is in operation which produces an incomplete counterbalancing of the deflections produced by topography, leaving much smaller deflections in the same direction. The deflections of the vertical are due to irregularities in the distribution of the masses composing the earth. These irregularities may occur either as a result of irregularities in the surface of the earth (topography), or as a result of irregularities in the distribution of the densities beneath the surface.

The distribution of the densities below the surface of the earth is invisible and largely unknown, but the theory of Isostasy postulates precisely such a relation between sub-surface densities and surface elevations.

If the earth were composed of homogeneous material, its figure of equilibrium, under the influence of gravity and its own rotation, would be an ellipsoid of revolution.

The earth though is composed of heterogeneous material which varies considerably in density. If this heterogeneous material were so arranged that its density at any point simply depended upon the depth of that point below the surface, or, more accurately, if all the material lying at each equipotential surface (rotation considered) was of one density, a state of equilibrium would exist and there would be no tendency toward a rearrangement of masses.

If the heterogeneous material composing the earth were not arranged in this manner at the outset, the stresses produced by gravity would tend to bring about such an arrangement, but because the material is not a perfect fluid, the rearrangement will be imperfect. In the partial

RING	Outer Radius (KM)	RING	Outer Radius (KM)
1	.0080	36	3.9211
2	.0095	37	4.6803
3	.0114	38	5.5865
4	.0136	39	6.6682
5	.0162	40	7.9592
6	.0194	41	9.5003
7	.0231	42	11.3398
8	.0276	43	13.5354
9	.0330	44	16.1562
10	.0393	45	19.2844
11	.0470	46	23.0184
12	.0561	47	27.4754
13	.0669	48	32.7956
14	.0799	49	39.1461
15	.0953	50	46.7267
16	.1138	51	55.7757
17	.1358	52	66.5781
18	.1621	53	79.4741
19	.1935	54	94.8707
20	.2310	55	113.2545
21	.2757	56	135.2082
22	.3291	57	161.4304
23	.3928	58	192.7602
24	.4688	59	230.2080
25	.5596	60	274.9951
26	.6680	61	328.6057
27	.7973	62	392.8567
28	.9517	63	469.9958
29	1.1359	64	562.8462
30	1.3558	65	675.0283
31	1.6184	66	811.3203
32	1.9317	67	978.2927
33	2.3057	68	1185.5146
34	2.7522	69	1448.1099
35	3.2850	70	1793.1006

Table 4. - Ring Outer Radius

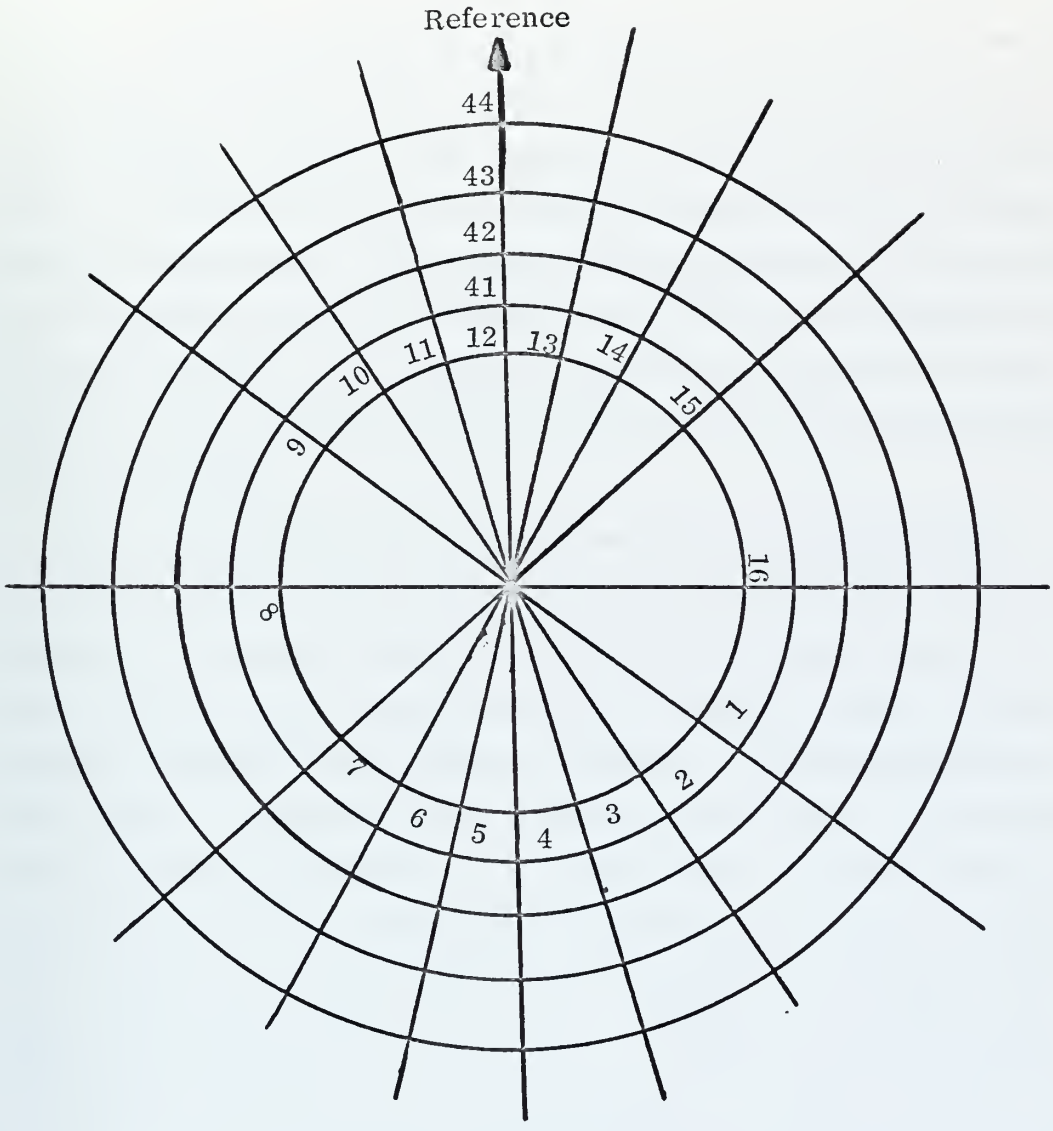

FIGURE 8. - Lunar Template

rearrangement some stresses will still remain as different positions of the same horizontal stratum may have somewhat different densities, and the actual surface of the earth will depart from the ellipsoid of revolution in the sense that above each region of deficient density there will be a bulge or bump, and above each region of excessive density there will be a hollow. The bumps on the earth would be mountains and the hollows would be ocean floors. The excess material represented by that portion of the mountains above the reference surface will be compensated for by a defect of density in the underlying material and vice-versa for the oceans. This, of course, can be explained by the famous Pratt-Hayford theory of Isostasy.

If we now consider the moon, we see that the consequences of hydrostatic theory as stated by Kopal [15] demand that given a sufficiently long time the material which on a short time-scale may behave as a solid is bound to get crushed under its own weight to settle to a form of minimum potential energy, which is a sphere. The departures of the lunar globe from spherical form permissible for a figure of equilibrium in the prevailing field of force are indeed small. To this extent, the moon may seem to be in hydrostatic equilibrium. However, this agreement becomes noticeably worse when we compare the momenta of the lunar globe with their theoretical values. Finally, by considering the mechanical ellipticity, we see that its value is so much at variance with the requirements of hydrostatic equilibrium that the discrepancy must be considered as real.

Therefore, in spite of the approximate prevalence of hydrostatic equilibrium in the lunar interior, as attested by the nearly spherical form of its globe, the moon's motion around its center of gravity reveals the presence of small but unmistakable departures from this equilibrium. On the other hand, O'Keefe [19] was able to show by comparison between calculated Bouguer anomalies and the essentially free air anomalies of Muller and Sjogren, that the topography of the moon could be isostatically

compensated and that to a rough first approximation the moon is in isostatic equilibrium. He considers an actual crustal layer on the moon, for which he states the Pratt-Hayford theory of Isostasy could be applied.

Under the assumption of Pratt's hypothesis of Isostasy, we will introduce a surface of compensation at the depth T below the reference surface. If we denote the changes of $\Delta\xi$ and $\Delta\eta$ due to the changes in topography by $\Delta\xi_o$ and $\Delta\eta_o$, then the sums $\Delta\xi + \Delta\xi_o$ and $\Delta\eta + \Delta\eta_o$ are the terms which, when summed, give the total deflection of the vertical. From Jordan-Eggert [11]:

$$\Delta\xi_o = \frac{-3\Delta\Theta T\rho''}{4\pi\Theta_m A}(\sin\alpha_2 - \sin\alpha_1)\log_e\left(\frac{r_2+\sqrt{T^2+r_2^2}}{r_1+\sqrt{T^2+r_1^2}}\right)$$

$$\Delta\eta_o = \frac{3\Delta\Theta T\rho''}{4\pi\Theta_m A}(\cos\alpha_2 - \cos\alpha_1)\log_e\left(\frac{r_2+\sqrt{T^2+r_2^2}}{r_1+\sqrt{T^2+r_1^2}}\right)$$

$$\Delta\Theta\Gamma = \Theta H$$

Therefore:

$$\Delta\xi_o + \Delta\xi = \frac{3\Theta H\rho''}{4\pi\Theta_m A}(\sin\alpha_2 \quad \sin\alpha_1)\left[\log_e\frac{r_2}{r_1} - \log_e\left(\frac{r_2+\sqrt{T^2+r_2^2}}{r_1+\sqrt{T^2+r_1^2}}\right)\right]$$

$$\text{let } F = \frac{\Delta\xi_o + \Delta\xi}{\Delta\xi} = 1 - \left(\frac{\log_e\left(\frac{r_2+\sqrt{T^2+r_2^2}}{r_1+\sqrt{T_2+r_1^2}}\right)}{\log_e\frac{r^2}{r_1}}\right)$$

Then for a definite value of T we can set up a table, from which for every value r_1 (because r_2 = constant $X r_1$) the factor F can be taken. Then we will have

$$\Delta\xi + \Delta\xi_o = F\Delta\xi$$

$$\Delta\eta + \Delta\eta_o = F\Delta\eta$$

O'Keefe states [19] that for 20% difference in lunar crust and lunar mantle density, a depth of compensation of 25 kilometers is in order, while for 10% difference, a depth of compensation of 50 kilometers is in order. Further extending these assumptions, calculations for depths of compensation of 25, 50, 75 and 100 kilometers has been made using the program and subprogram in Appendix A.

Table 5 gives the various F factors for each ring owing to a specific assumed depth of compensation.

Calculations have also been made for 125, 250, 500, 1,000 and 1,500 kilometers depth of compensation primarily to obtain a full set of values.

There is direct evidence of excess mass in the maria over what would be called for by Isostasy. The explanation of this excess mass which was discovered by Muller and Sjogren of JPL is subject to various interpretations. O'Keefe [19] states that this excess mass may be due to the maria being filled with some sort of material which arrived after the formation of the highland topography. H. C. Urey [21] states that this mascon effect could be produced by a flat circular slab of chrondritic material. For instance, Urey calculated that in Mare Imbrium, this disc would be some 4 kilometers thick and be 670 kilometers in diameter (mass = 5 X 10^{21} grams).

J. G. Stipe [20] states that these mascons could be caused by meteorites which have bombarded the moon and have been of necessary size and at necessary depth to create these mass anomalies.

RING	25 km	50 km	75 km	100 km
2	0.9997	0.9998	0.9999	0.9999
3	0.9996	0.9998	0.9999	0.9999
4	0.9995	0.9998	0.9998	0.9999
5	0.9994	0.9997	0.9998	0.9999
6	0.9993	0.9996	0.9998	0.9998
7	0.9992	0.9996	0.9997	0.9998
8	0.9990	0.9995	0.9997	0.9998
9	0.9988	0.9994	0.9996	0.9997
10	0.9986	0.9993	0.9995	0.9996
11	0.9983	0.9991	0.9994	0.9996
12	0.9979	0.9990	0.9993	0.9995
13	0.9975	0.9988	0.9992	0.9994
14	0.9971	0.9985	0.9990	0.9993
15	0.9965	0.9983	0.9988	0.9991
16	0.9958	0.9979	0.9986	0.9990
17	0.9950	0.9975	0.9983	0.9988
18	0.9941	0.9970	0.9980	0.9985
19	0.9929	0.9965	0.9976	0.9982
20	0.9915	0.9958	0.9972	0.9979
21	0.9899	0.9949	0.9966	0.9975
22	0.9879	0.9940	0.9960	0.9970
23	0.9856	0.9928	0.9952	0.9964
24	0.9828	0.9914	0.9943	0.9957
25	0.9795	0.9897	0.9932	0.9949
26	0.9755	0.9878	0.9918	0.9939
27	0.9708	0.9854	0.9903	0.9927
28	0.9651	0.9826	0.9884	0.9913
29	0.9584	0.9792	0.9861	0.9896
30	0.9504	0.9752	0.9834	0.9876
31	0.9408	0.9704	0.9802	0.9852
32	0.9294	0.9646	0.9764	0.9823
33	0.9158	0.9578	0.9718	0.9789
34	0.8996	0.9496	0.9664	0.9748
35	0.8804	0.9399	0.9599	0.9699

Table 5. - F Factors

Table 5. - F Factors (Continued)

RING	25 km	50 km	75 km	100 km
36	0.8577	0.9283	0.9521	0.9641
37	0.8309	0.9145	0.9429	0.9571
38	0.7994	0.8981	0.9319	0.9489
39	0.7627	0.8787	0.9188	0.9390
40	0.7200	0.8556	0.9032	0.9272
41	0.6712	0.8285	0.8847	0.9133
42	0.6163	0.7965	0.8627	0.8966
43	0.5558	0.7593	0.8368	0.8769
44	0.4908	0.7161	0.8063	0.8535
45	0.4232	0.6669	0.7707	0.8260
46	0.3557	0.6115	0.7293	0.7936
47	0.2910	0.5505	0.6818	0.7559
48	0.2319	0.4852	0.6282	0.7122
49	0.1803	0.4175	0.5687	0.6624
50	0.1370	0.3501	0.5045	0.6065
51	0.1022	0.2858	0.4373	0.5451
52	0.0751	0.2272	0.3695	0.4795
53	0.0545	0.1763	0.3040	0.4118
54	0.0392	0.1338	0.2435	0.3445
55	0.0280	0.0996	0.1902	0.2806
56	0.0199	0.0731	0.1452	0.2225
57	0.0141	0.0530	0.1086	0.1722
58	0.0099	0.0381	0.0800	0.1304
59	0.0070	0.0272	0.0582	0.0969
60	0.0049	0.0193	0.0418	0.0710
61	0.0035	0.0136	0.0299	0.0513
62	0.0024	0.0096	0.0212	0.0368
63	0.0017	0.0067	0.0150	0.0262
64	0.0012	0.0047	0.0105	0.0185
65	0.0008	0.0033	0.0074	0.0130
66	0.0006	0.0023	0.0051	0.0091
67	0.0004	0.0016	0.0035	0.0063
68	0.0003	0.0011	0.0024	0.0043
69	0.0002	0.0007	0.0016	0.0029
70	0.0001	0.0005	0.0011	0.0019

Wise and Yates [22] state that mascons are produced by mantle plugs upwelling into giant impact bases punched through the lunar crust, followed by volcanic filling of the remainder of the crater above the plug.

No matter which theory is accepted, the direct result will be a further deflection of the vertical. The area where the mascon is located, will deflect the vertical, proportionately larger than the height of this area would indicate. The exact numerical increase in the deflection would be dependent upon the mass distribution as offered in the theories above. We could consider these mass increases as additional point masses and compute their effect on the deflections accordingly, or we could select a station which would minimize their effect.

Let us consider a central station which is quite distant from the major mass anomalies so that their effect will be insignificant (very low F factor) in the overall result. For instance, considering any station near the equator from 20° east longitude westward to 40° west longitude will limit the contribution of these mass anomalies on the deflection of the vertical as the station will be greater than 600 kilometers from the outer edge of these anomalies. We can see for a station greater than 600 kilometers from a large mass anomaly that the largest F factor is only about .015 (down to 100 km compensation depth) and the contribution of the mass anomalies are then generally negligible on the overall result. For topographic deflections only, the area of these mass anomalies will generally fall into one compartment only, and will in turn affect the result very little. For this reason, I have selected the center of the crater Landsberg "A" as a starting point. Its coordinates are 328° 57'W and 0° 13'N. This point was also selected due to availability of charts. Due to the nearly concentric area in terms of height of the center of Landsberg "A" and the use of a 1:250,000 chart, I have neglected rings 1 to 35, which are approximately the inner 3 kilometers of rings. Rings 36 to 50 were computed using the AMS series topographic lunar map sheet 1 edition 1 of 3 - 64. This map is a modified stereographic projection

with a point of origin 4,410.10 kilometers from the point of tangency of the map plan and a selenographic sphere with a radius of 1,737.988 kilometers. The contour interval is 250 meters based on a vertical datum centered at Mösting "A" at an elevation of 7,000 meters. The horizontal datum was also based on the center of Mösting "A" which was considered to be latitude 3° 10' 47" S and longitude 354° 50' 13". Rings 51 to 63 were computed using an edition 1 - AMS sheet 2 topographic lunar map, scale 1:2,000,000 with the same datum, etc., as above. Rings 64 to 68 were computed using an edition 2 - AMS sheet 2 topographic lunar map, scale 1:5,000,000 with the same datum, etc., as above.

Rings beyond 68 were neglected due to their approach to the lunar limb; and their coinciding reduction in accuracy of height determination.

Tables 6 and 7 give the heights of each compartment for computations in the prime vertical and in the meridian respectively.

Table 8 shows the computed deflections for assumed depths of compensation.

RING	ZONE																
	1	2	3	4	5	6	7	8	9	10	11	12	13	14	15	16	ξ
36	8350	8275	8275	8250	8250	8250	8250	8250	8250	8125	8125	8200	8200	8200	8250	8400	- .475
37	8250	8175	8175	8150	8150	8150	8150	8150	8150	8100	8100	8125	8250	8250	8250	8300	+ .150
38	8100	8050	8050	8025	8000	8000	8000	8025	8050	8000	8050	8050	8125	8125	8125	8125	+ .400
39	7950	7950	7950	7925	7900	7900	7900	7925	7950	7950	7975	8000	7975	7975	7950	7950	+ .325
40	7950	7925	7925	7900	7850	7850	7875	7900	7925	7925	7925	7950	7950	7950	7950	7950	+ .350
41	7900	7875	7850	7800	7750	7750	7775	7825	7850	7825	7800	7825	7850	7875	7900	7900	+ .300
42	7800	7775	7725	7600	7550	7600	7650	7750	7800	7800	7775	7775	7775	7800	7825	7850	+ .950
43	7775	7775	7650	7550	7500	7500	7550	7650	7750	7750	7725	7750	7750	7775	7775	7800	+1.125
44	7800	7750	7625	7500	7400	7375	7500	7600	7700	7625	7575	7550	7625	7750	7775	7775	+ .825
45	7800	7650	7550	7350	7300	7250	7300	7450	7600	7550	7450	7425	7500	7625	7700	7750	+ .950
46	7775	7650	7450	7275	7150	7125	7125	7300	7500	7350	7300	7350	7350	7525	7525	7750	+ .700
47	7850	7600	7350	7200	7050	7025	7025	7200	7250	7125	7100	7150	7375	7550	7650	7750	+ .650
48	7850	7600	7300	7100	7000	7000	7000	7100	7100	7050	7050	7150	7500	7550	7600	7700	+ .750
49	7800	7625	7250	7000	7000	7000	7000	7000	7000	7000	7000	7100	7500	7550	7650	7700	+ .825
50	7950	7625	7500	7150	7000	7000	7000	7000	7000	7000	7000	7250	7500	7500	7650	7750	+ .425
51	7500	7500	7600	7300	7000	7000	7000	7000	7000	7000	7000	7000	7000	7500	7500	7500	- .400
52	7600	7800	8000	7500	7250	7000	7000	7000	7000	7000	7000	7000	7250	7250	7250	7400	-2.00

Table 6. - Compartment Heights for Computations in the Meridian

RING

ZONE

	1	2	3	4	5	6	7	8	9	10	11	12	13	14	15	16	ξ
53	7500	7500	7800	7800	7500	7000	6900	6900	6900	6900	6900	6900	7400	7000	7200	7500	- 2.10
54	7600	7600	7500	7500	7500	7100	6900	6900	6900	6900	6900	6900	7000	7000	7000	7400	- 2.50
55	7500	7500	7600	7600	7600	7000	6900	6900	6900	6800	7200	7100	7000	6900	6900	7200	- 2.60
56	7600	7300	7300	7300	7300	7100	7000	7000	6900	6800	7200	7000	7000	6900	6900	7500	- 1.70
57	7500	7300	7300	7300	7300	7200	7200	7100	6900	6800	6900	6900	6900	6900	6900	7200	- 2.80
58	7300	7300	7300	7300	7300	7300	7300	7200	6900	6800	6900	6900	6900	6900	6900	7100	- 3.00
59	7200	7300	7300	7300	7300	7300	7200	6900	6900	6900	6900	6900	6900	7100	7100	7200	- 1.90
60	7300	7300	7400	7300	7400	7400	7200	7000	6800	6900	6900	6900	6900	6900	7000	7500	- 2.50
61	7800	7400	7600	7400	7400	7100	7100	6700	6800	6900	6900	6900	6900	7000	7200	8000	- 1.90
62	7600	7400	7400	7400	7400	7000	6900	6700	6400	6500	6800	6800	6900	7000	7300	7900	- 2.20
63	7200	7400	7400	7400	7400	7300	6900	6300	6200	6400	6500	6800	7100	7300	8200	7900	- .90
64	7700	7600	7500	7500	7500	7400	6800	5700	6000	6000	6500	6500	7000	7800	8500	7900	- 1.50
65	7700	7700	7500	7500	7200	7400	7200	6400	5600	5500	5700	6000	6700	7000	7500	7600	- 7.00
66	7700	7700	7600	7400	7000	7200	7300	6000	5400	5500	5500	5800	6200	6200	6600	7500	- 9.20
67	6800	7700	7700	7400	6800	7500	7300	5900	5300	5500	5400	5300	5500	5600	6200	7500	- 12.60
68	8500	8200	8400	7500	7600	7500	7400	6000	5100	5100	5400	5300	4900	5200	6400	7000	- 15.90

ξ = - 1'04".45

Table 6. - (Continued)

RING	ZONE																
	1	2	3	4	5	6	7	8	9	10	11	12	13	14	15	16	η
36	8250	8250	8250	8250	8250	8200	8175	8150	8200	8300	8400	8350	8375	8350	8325	8275	+ .800
37	8150	8150	8175	8150	8175	8150	8125	8100	8250	8250	8300	8275	8275	8250	8225	8175	+ .825
38	8000	8000	8025	8000	8025	8050	8025	8050	8125	8125	8125	8125	8125	8100	8075	8050	+ .675
39	7900	7900	7925	7950	7950	7950	7950	7975	7975	7950	7950	7950	7950	7950	7950	7950	+ .125
40	7850	7875	7900	7925	7925	7925	7925	7925	7950	7950	7950	7950	7950	7950	7950	7925	+ .325
41	7750	7800	7825	7850	7850	7850	7825	7825	7875	7900	7900	7875	7900	7900	7900	7850	+ .525
42	7600	7700	7750	7775	7775	7800	7800	7775	7800	7825	7850	7825	7825	7800	7775	7725	+ .500
43	7500	7600	7650	7700	7750	7750	7750	7750	7775	7775	7800	7775	7775	7775	7775	7675	+ .675
44	7400	7550	7600	7650	7650	7700	7650	7600	7700	7775	7775	7800	7800	7800	7750	7625	+1.225
45	7300	7350	7450	7550	7550	7600	7550	7475	7600	7725	7750	7775	7800	7800	7700	7550	+1.875
46	7125	7200	7300	7400	7450	7500	7400	7300	7450	7600	7750	7775	7775	7750	7650	7450	+2.525
47	7025	7100	7200	7250	7250	7250	7150	7125	7500	7650	7750	7800	7800	7850	7700	7400	+4.10
48	7000	7050	7100	7100	7100	7100	7100	7100	7550	7600	7700	7800	7800	7850	7700	7350	+4.70
49	7000	7000	7000	7000	7000	7000	7000	7050	7550	7650	7700	7750	7750	7800	7650	7325	+5.25
50	7000	7000	7000	7000	7000	7000	7000	7050	7550	7700	7750	7850	7900	7950	7650	7500	+5.80
51	7000	7000	7000	7000	7000	7000	7000	7000	7400	7500	7500	7500	7500	7500	7500	7500	+3.90
52	7100	7000	7000	7000	7000	7000	7000	7000	7250	7300	7400	7500	7600	7600	7700	7800	+4.05

Table 7. - Compartment Heights for Computations in the Prime Vertical

RING	ZONE																
	1	2	3	4	5	6	7	8	9	10	11	12	13	14	15	16	η
53	7100	6900	6900	6900	6900	6900	6900	6900	7000	7300	7500	7500	7500	7500	7500	7700	+ 4.10
54	7100	6900	6900	6900	6900	6900	6900	6900	6900	7300	7400	7500	7600	7600	7600	7600	+ 4.10
55	7100	6900	6900	6900	6900	6900	6900	7000	6900	7000	7200	7500	7500	7500	7500	7500	+ 3.10
56	7100	7000	7000	6900	6900	6900	6900	7000	6900	7000	7500	7500	7600	7600	7500	7300	+ 3.20
57	7200	7200	7100	7000	7000	6900	6900	6900	6900	7000	7200	7400	7400	7500	7400	7300	+ 1.90
58	7300	7200	7100	7000	6900	6900	6900	6900	7000	7100	7200	7200	7200	7300	7300	7300	+ 0.70
59	7300	7100	6900	6900	6900	6900	6900	6900	7000	7100	7200	7200	7200	7200	7300	7300	+ 1.70
60	7300	7100	7000	6900	6900	6800	6900	6900	6900	7200	7500	7400	7400	7300	7300	7400	+ 2.60
61	7200	7000	6700	6700	6800	6800	6800	6900	7000	7500	8000	7900	8000	7800	7600	7500	+ 6.20
62	7100	6800	6700	6600	6500	6400	6500	6700	7100	7300	7900	7700	7700	7600	7500	7400	+ 6.70
63	7200	6500	6300	6200	6200	6200	6400	6600	7500	8000	7900	7500	7400	7200	7300	7400	+ 8.60
64	7200	6000	5700	5900	6000	6000	6000	6400	7800	8200	7900	7800	7800	7700	7600	7500	+ 13.10
65	7300	6700	6400	6200	6100	5600	5700	5800	7100	7600	7600	7600	7700	7700	7700	7600	+ 10.80
66	7200	6500	6000	5700	5600	5400	5500	5600	6400	7200	7500	7600	7700	7700	7700	7600	+ 11.90
67	7200	6400	5900	5700	5600	5300	5400	5400	5800	6900	7500	7800	8200	8600	8100	7600	+ 13.60
68	7500	6600	6000	5400.	5300	5100	5300	5300	5600	6700	7000	7800	8200	8500	8100	8000	+ 13.60

η = 2' 17".48

Table 7. - (Continued)

Compensation Depth	ξ	η
25 km	+ 2".934	+ 10".983
50 km	+ 3".332	+ 20".709
75 km	+ 2".234	+ 27".757
100 km	+ 0".883	+ 33".123
125 km	- 0".547	+ 37".447
250 km	- 6".118	+ 49".548
500 km	- 16".792	+1' 11".984
1,000 km	- 30".184	+1' 38".947
1,500 km	- 38".529	+1' 47".427
∞	-1'04".450	+2' 17".480

Table 8. - Deflections Considering Depths of Compensation

We cannot consider that the value of Θ will remain constant down to the depths which we are considering. Thus, as depths increase, the average density for this surface layer will vary. We consider that the average density for these depths are as follows in Table 9 (interpolated from Kaula [12]).

KM	Average Density	F1
25	2.670	1
50	3.000	1.1236
75	3.140	1.1760
100	3.210	1.2022
125	3.250	1.2171
150	3.263	1.2221
250	3.336	1.2494
500	3.343	1.2521
1,000	3.300	1.2360
1,500	3.343	1.2521

Table 9. - Average Surface Density for Selected Depth

The F1 factor in Table 9 is a deflection multiplier, and its effect on deflections is given in Table 10.

Compensation Depth	ξ	η
25 km	+ 2".934	+ 10".983
50 km	+ 4".118	+ 23".269
75 km	+ 2".627	+ 32".642
100 km	+ 1".062	+ 39".820
125 km	- 0".666	+ 45".447
250 km	- 7".644	+1'01".905
500 km	- 21".025	+1'30".131
1,000 km	- 37".307	+2'02".298
1,500 km	- 48".242	+2'14".509
∞	- 1'04".450	+2'17".480

Table 10. - Deflections Considering Changes in Density for Changes in Depth of Compensation

The graph in Figure 10 shows the relationship of depth of compensation to deflections, considering no change in surface density, and considering a change in the surface density for changes in the depth of compensation.

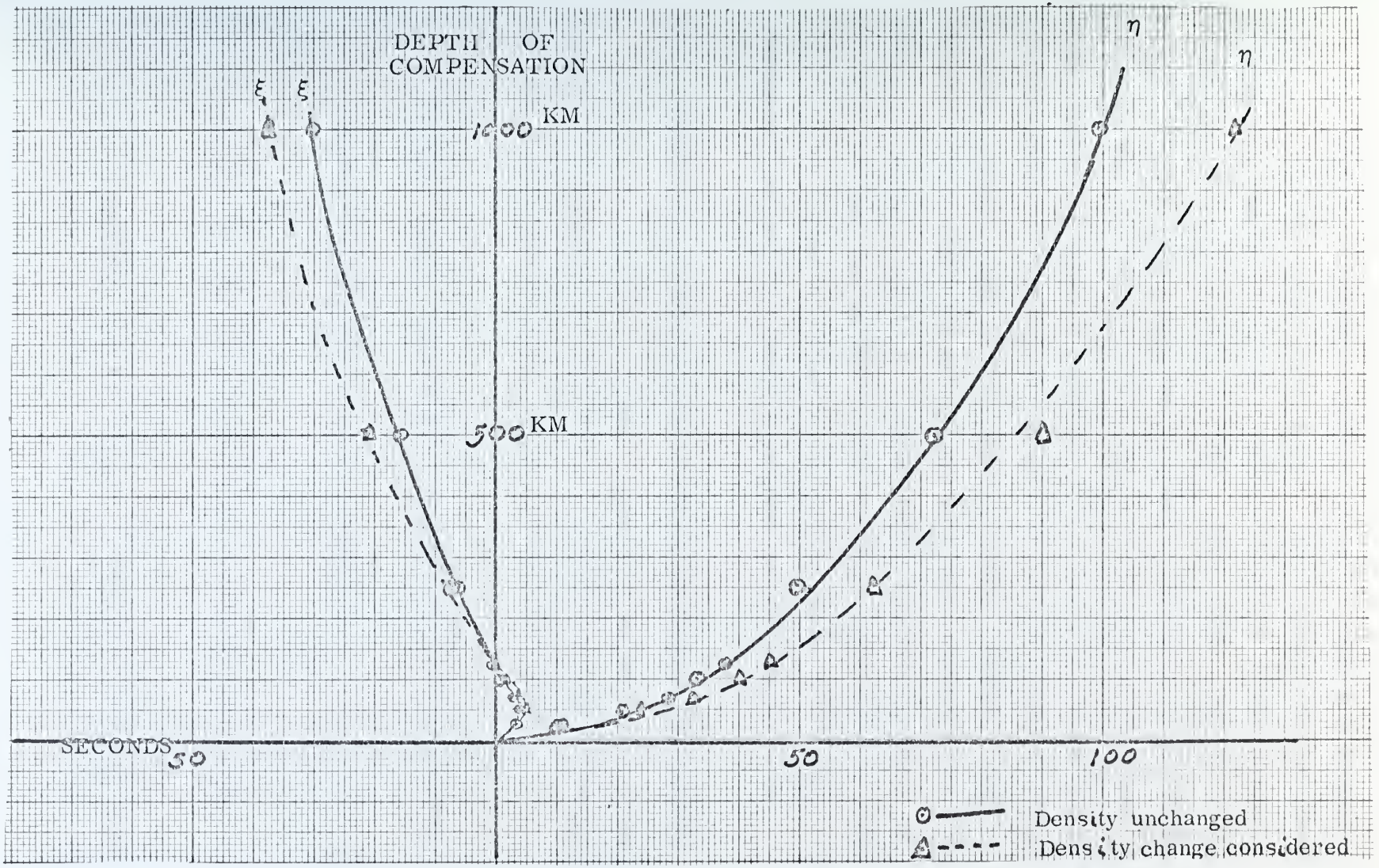

Figure 9. - Deflections Considering Changes in Density for Changes in Depth of Compensation

The maximum topographic deflections on the moon will most likely occur at a highland-maria dividing line. For instance, a north-south deflection was examined at the southern wall of the crater Pitatus at latitude $31^{\circ}10'$ S and longitude $346^{\circ}10'$. With a few assumptions (due to lack of large scale charts on the area) it was determined that this deflection was approximately 5 minutes. It is quite possible that other larger deflections exist, but probably will not greatly exceed this value. It is interesting to note that the deflections may be greatly minimized by choosing a station which is surrounded by nearly concentric rings of equal elevation. This will yield nearly zero deflections for the inner zones. This ideal station could be at the center of a concentric crater, at the top of an isolated rise on flat ground, or at a central point of a flat area. If, of course, a station were selected which did not satisfy this concentric condition, the inner rings must be considered.

3.2 Computation of Spherical Harmonic Deflections of the Vertical

In order to compare the values obtained by the method of isostatic-topographic deflections, we will use the formula as given by Dragg [3] to compute the deflections by the use of spherical harmonics.

$$\xi = \frac{-1}{\gamma \cos\varphi} \sum_{N=2}^{\infty} \sum_{M=0}^{N} (A_{NM} \cos M\lambda + B_{NM} \sin M\lambda) \left[\frac{N+1}{N-1} P_{NM}(\sin\varphi) \cdot \sin\varphi - \frac{(N-M+1)}{N-1} P_{N+1,M}(\sin\varphi) \right]$$

$$\eta = \frac{1}{\gamma \cos\varphi} \sum_{N=2}^{\infty} \sum_{M=0}^{N} \frac{M}{N-1} (A_{NM} \sin M\lambda - B_{NM} \cos M\lambda) P_{NM}(\sin\varphi)$$

Dragg [3] neglected the 20, 21, and 40 spherical harmonic terms in his computation for the earth, but they have been included in this paper.

I will use the spherical harmonics coefficients given by Blackshear [6], (see Appendix D). These are C_{NM} and S_{NM} coefficients which must be converted to A_{NM} and B_{NM} above.

By definition we see that $C_{NM} = J_{NM}$ and $S_{NM} = K_{NM}$.

For Heiskanen and Moritz [9], we see

$$A'_{NM} = GM\, r^N\, J_{NM}$$

$$B'_{NM} = -GM\, r^N\, K_{NM}$$

and that from Dragg [3]

$$A_{NM} = \frac{(N-1)}{r^{N+2}}\, A'_{NM}$$

$$B_{NM} = \frac{(N-1)}{r^{N+2}}\, B'_{NM}$$

Thus we see that in terms of coefficients C_{NM} and S_{NM}

$$\xi = \frac{1}{\cos\varphi} \sum_{N=2}^{\infty} \sum_{M=0}^{N} (C_{NM}\cos M\lambda + S_{NM}\sin M\lambda) \left[(N+1)\, P_{NM}(\sin\varphi) \cdot \sin\varphi - (N-M+1)\, P_{N+1,M}(\sin\varphi)\right]$$

$$\eta = \frac{-1}{\cos\varphi} \sum_{N=2}^{\infty} \sum_{M=0}^{N} M(C_{NM}\sin M\lambda - S_{NM}\cos M\lambda)\, P_{NM}(\sin\varphi)$$

This equation was evaluated for the Landsberg "A" station using the IBM 360-75 computer, the program of which is contained in Appendix B.

The results of this evaluation are

$$\xi = -12'.184$$

$$\eta = 2'13''.707$$

These values fall between the isostatic-topographic results of 250 km depth of compensation, and the results of topographic compensation only,

when surface density changes are not considered. These values fall between the isostatic-topographic results of 250 km and 1,500 km depths of compensation, when surface density changes are considered.

3.3 Effect of Other Bodies on the Deflection of the Vertical

It is obvious that the attractive effect of the sun and the earth will affect the deflection of the vertical on the lunar surface. The following developments refer directly to the earth but apply equally as well to the sun. Planets also have an effect but for all practical purposes this effect can be considered insignificant.

Following the method of Jordan-Eggert [11] adapted for the moon, we see that

$$\text{Deflection} = \frac{3\, M_e\, A^3 \sin Z \cos Z}{M_m\, r^3}$$

where

M_e - The mass of the earth

M_m - The mass of the moon

A - The lunar radius

Z - Zenith Distance of the earth

r - Earth-moon distance

and where $\frac{M_e}{M_m} = 81.301$

and $\frac{A^3}{r^3} = \frac{(1737.63)^3}{(384,400)^3} = 9.27 \times 10^{-8}$

Therefore:

$$\text{Deflection} = 2.253 \times 10^{-5}\, \rho'' \sin Z \cos Z$$
$$= 4''.646912274 \sin Z \cos Z$$
$$= 2''.323 \sin 2Z$$

For the effect of the sun we will use the formula

$$\text{Deflection} = \frac{3\, M_s\, A^3 \sin Z \cos Z}{M_m\, r^3}$$

Where $\frac{M_s}{M_m} = 27{,}158{,}000$

and $\frac{A^3}{r^3} = \frac{(\ 1{,}737.63\ )^3}{(149{,}415{,}834.4)^3} = 1.5728 \times 10^{-15}$

$$\text{Deflection} = 0''.026 \sin Z \cos Z$$
$$= 0''.013 \sin 2Z$$

which is negligible in comparison with other uncertainties introduced.

We will now divide the deflection of the vertical caused by the earth's attraction into a northward and westward directed component. If A is the azimuth of the earth counted from the north, then we have for the two components of the deflection of the vertical

$$\xi_e = 2''.32 \sin 2Z \cos A$$

$$\eta_e = 2''.32 \sin 2Z \sin A$$

These deflections are not constant for a station but vary in accordance with the change in earth-moon distance and the geometric librations in latitude and longitude. They also vary with the physical librations but these are insignificant.

3.4 Conclusions

Due to lack of knowledge of the lunar interior and its isostatic properties, we cannot, with any degree of confidence, state the magnitude of the deflections of the vertical at a given point.

For the computation of the topographic deflections, we used lunar charts with a lunar centered spherical surface as the equipotential

reference surface, and from these the compartment relative heights were determined. If we consider the effect of an offset sphere on this computation, we can see immediately that the relative heights would change in accordance with the translation of the sphere's center. For instance, if the center of the reference sphere were offset toward the earth, the relative heights of the eastern compartments calculated in this paper would be considerably less, and the η deflections, considerably smaller. Thus, we will need better height determination on the moon, before the topographic deflections can be considered to be sufficiently accurate. Due to the relative ease of computation of the spherical harmonic deflections, it may be best to use them at present instead of the topographic deflections, especially in areas which have local concentric heights. The computed deflections could be, of course, corrected for the effect of the earth.

If in the future, Method (1) is employed, and relative deflections between stations were obtained, we would be in a much better position to predict the absolute deflections at these same stations using the topographic method.

The employment of Method (2) would, if extensive enough, yield the absolute deflections of each station. It is considered that in this method, lies the best possible results. But, alternately, the most time and effort would be required over the other methods.

Further work can be accomplished using Method (3). For instance, Karl Jung in Report No. 41 of The Ohio State University, Institute of Geodesy, Photogrammetry and Cartography, has given the formulas to obtain approximate values of the influence of lunar craters on the deflection. These computations could become particularly useful for stations offset from the crater centers, as they would yield a rapid evaluation of the deflection attributed to the inner rings of the template.

BIBLIOGRAPHY

1. Carroll, J. E., (1969). An Automatic Instrument for the Determination of Astro-Azimuth. AIAA Paper No. 69-861, AIAA Guidance, Control, and Flight Mechanics Conference, Princeton, New Jersey, August 18-20, 1969.

2. Carroll, J. E., (1969). "A New Instrument for the Determination of Astronomic Position", Surveying and Mapping, Vol. XXIX, No. 3, September, 1969.

3. Dragg, J., (1963). Application of Spherical Harmonics to Geodetic Problems, Aeronautical Chart and Information Center, Department of Defense, St. Louis, Missouri, Reference Publication #15.

4. Grumman Company, ( ), LM Optical Subsystem, Manuscript.

5. Gurevich, V. B., (1967). "Astronomical Determination of Position on the Moon", Soviet Astronomy - AJ, V. 11, No. 1, January-February, 1967.

6. Haines, E., (1969). Lunar Scientific Model, Jet Propulsion Laboratory, Pasadena, California, Document No. 900 - 278, Volume I.

7. Geonautics, Inc., (1965). Study of Selenodetic Measurements for Early Apollo Missions, Final Report Contract No. NAS 9-2803.

8. Hayford, J. F., (1909). The Figure of the Earth and Isostasy from Measurements in the United States, Department of Commerce and Labor, Coast and Geodetic Survey, Special Publication No. 82.

9. Heiskanen, W. A., and Moritz, H., (1967). Physical Geodesy, San Francisco, W. H. Freeman and Company.

10. Jet Propulsion Laboratory, ( ). Kalman Filter, JPL Technical Report No. 32 - 498.

11. Jordan - Eggert, (1941). Handbuch der Vermessungskunde, Volume III, Second Half, English Translation by Carta, M.W., 1962.

12. Kaula, W. M., (1968). An Introduction to Planetary Physics/The Terrestrial Planets, John Wiley and Sons, Inc., New York.

13. Kokurin, YU. L., Karbason, V.V., Lobanov, U.F., Suhanovsky, A.N., Chernykh, N.S., (1968). "Possibilities for Improving Certain Astronomical Parameters of the Earth-Moon System by the Optical Radar Method", Kosmcheskie Issledovaniya, Volume 5, No. 2, pp. 219-224, March - April.

14. Kolaczek, B., (1968). Selenocentric and Lunar Topocentric Spherical Coordinates, Smithsonian Astrophysical Observatory Cambridge, Massachusetts, Special Report 286.

15. Kopal, Zdenek, (1969). The Moon, D. Reidel Publishing Company, Dordrecht, Holland.

16. Mueller, I. I., (1969). Spherical and Practical Astronomy as Applied to Geodesy, Frederick Ungar Publishing Company, New York.

17. Nassau, J. J., (1948). Practical Astronomy, McGraw - Hill Book Company, Inc., New York.

18. Norton, A. P., Inglis, J. G., (1964). Norton's Star Atlas, Sky Publishing Corporation, Cambridge, Massachusetts.

19. O'Keefe, J. A., (1968). "Isostasy on the Moon", Science, Vol. 162, pp. 1405-1406.

20. Stipe, J. G., (1968). "Iron Meteorites as Mascons", Science, Vol. 162, pp. 1402-1403.

21. Urey, H. C., (1969). "The Contending Moons", Astronautics and Aeronautics, Vol. 7, No. 1, January, 1969.

22. Wise, D. U., and Yates, M. T., (1970). "Mascons as Structural Relief on a Lunar Moho", Journal of Geophysical Research, Vol. 75, January 10, pp. 261-268.

APPENDIX A

F FACTOR COMPUTATION PROGRAM AND ASSOCIATED MOON CURVATURE SUB-PROGRAM

The main program computes the "F" factor for a given ring, given the depth of compensation. The associated sub-program computes the change in outer ring radius due to moon curvature. The main program list of variables is:

IR	Indexing variable for ring number
J	Indexing variable and integer compensation depth
A1	Inner radius of ring
A2	Outer radius of ring
T	Real number compensation depth
FA	Compensation depth squared plus outer radius squared
FB	Compensation depth squared plus inner radius squared
FC	Outer radius plus the square root of FA
FD	Inner radius plus the square root of FB
FE	FC divided by FD
FF	The natural log of FE
FG	The outer radius divided by the inner radius
FH	The natural log of FG
F	The F factor equal to 1 - FF/FH

The sub-program Mooncu uses an iterative procedure employing the secant method to compute the outer ring radius taking moon curvature into account.

The sub-program list of variables is:

THETA1	The inner radius divided by the lunar radius expressed in radians
THETA2	The outer radius uncorrected for lunar curvature expressed in radians
THETB2	An approximate outer radius corrected for curvature expressed in radians

T1	THETA 1/4
T2	THETA 2/4
T2B	THETB 2/4
T21B	Tangent of T2B
T21	Tangent of T2
T11	Tangent of T1
T3	T21/T11
T3B	T21B/T11
SOC	The natural log of T3 minus the cosine of $\frac{1}{2}$ THETA 1 plus the cosine of $\frac{1}{2}$ THETA 2 minus the natural log of the outer radius divided by the inner radius which is given by definition. This is considered the first approximation.
ASOC	The natural log of T3B minus the cosine of $\frac{1}{2}$ THETA 1 plus the cosine of $\frac{1}{2}$ THETB 2 minus the natural log of the outer radius divided by the inner radius which is given by definition. This is considered the second approximation.
THETC2	By the secant method where: $$X_{i+1} = \frac{X_{i-1}\, f(X_i) - X_i\, f(X_{i-1})}{f(X_i) - f(X_{i-1})}$$ we see $$\text{THETC2} = \frac{\text{THETA2 (ASOC)} - \text{THETB2 (SOC)}}{\text{ASOC} - \text{SOC}}$$
CSOC	The difference between X_{i+1} and X_i
BSOC	Outer radius in kilometers

MAIN

```
0001            DO 12 J=25,125,25
0002            WRITE(6,70)J
0003         70 FORMAT(1H0,5X,'BASED ON A DEPTH OF COMPENSATION OF',I4,'KILOMET')
0004            T=J
0005            IR=1
0006            WRITE(6,80)
0007         80 FORMAT(9X,'RING',10X,'F FACTOR',10X,'OUTER RADIUS')
0008            A1=.0080
0009         83 A2=1.19362053*A1
0010         88 FA=T**2+A2**2
0011            FB=T**2+A1**2
0012            FC=A2+SQRT(FA)
0013            FD=A1+SQRT(FB)
0014            FE=FC/FD
0015            FF=ALOG(FE)
0016            FG=A2/A1
0017            FH=ALOG(FG)
0018            F=1.-FF/FH
0019            IR=IR+1
0020            WRITE(6,84)IR,F,A2
0021         84 FORMAT(9X,I4,10X,F10.4,8X,F10.4)
0022            A1=A2
0023            IF(IR.LT.30) GO TO 83
0024            CALL MOONCU(A1,A2)
0025            IF(IR.GT.70) GO TO 12
0026            GO TO 88
0027         12 CONTINUE
0028            STOP
0029            END
```

MOONCU

```
0001               SUBROUTINE MOONCU(A1,BSOC)
0002               THETA1=A1/1737.63
0003            13 THETA2=1.19362053*THETA1
0004               THETB2=1.2*THETA1
0005               IF(THETA2.GT.1.) GO TO 12
0006            10 T2=THETA2/4.
0007               T2B=THETB2/4.
0008               T1=THETA1/4.
0009               T21B=TAN(T2B)
0010               T21=TAN(T2)
0011               T11=TAN(T1)
0012               T3=T21/T11
0013               T3B=T21B/T11
0014               SOC=ALOG(T3)-COS(THETA1/2.)+COS(THETA2/2.)-0.17699115
0015               ASOC=ALOG(T3B)-COS(THETA1/2.)+COS(THETB2/2.)-0.17699115
0016               THETC2=(THETA2*ASOC-THETB2*SOC)/(ASOC-SOC)
0017               CSOC=THETC2-THETB2
0018               BSOC=1737.630*THETC2
0019               IF(ABS(CSOC).LT.1.E-6) GO TO 12
0020               THETA2=THETB2
0021               THETB2=THETC2
0022               GO TO 10
0023            12 RETURN
0024               END
```

APPENDIX B

LEGENDRE POLYNOMIAL COMPUTATION PROGRAM AND SPHERICAL HARMONIC DEFLECTION PROGRAM

The program computes the Legendre polynomials and the deflections of the vertical in both the meridian and the prime vertical using the 13th degree polynomial coefficients as given by Blackshear [6] for the position of the center of Landsberg "A". The Legendre polynomials were computed to the fourteenth degree as required and the subscript 15 represents the 0th element [P(15,15) = P(0,0)]. The program list of variables is:

P(15,15)	An array which contains the Legendre polynomials
C(14,14)	An array which contains the Blackshear C coefficients
S(14,14)	An array which contains the Blackshear S coefficients
ALAT	Latitude of computation point
ALONG	Longitude of computation point
U	Sine of latitude
T	Cosine of latitude
I,J,KA,M	Indexing variables
MA,MB,N	Indexing variables
PSI	Evaluation of a single term of the deflection in the meridian
APSI	Sum of PSI Terms
PNU	Evaluation of a single term of the deflection in the prime vertical
APNU	Sum of PNU terms

PPSI	Multiplication of APSI by constants for final value of deflection in meridian
PPNU	Multiplication of APNU by constants for final value of deflection in prime vertical

```
0001            DIMENSION P(15,15),C(14,14),S(14,14)
0002            READ(5,20)C
0003            READ(5,20)S
0004         20 FORMAT(4E18.11)
0005            ALAT=.602151662
0006            ALONG=-.545415406
0007         99 U=SIN(ALAT)
0008            T=COS(ALAT)
0009            DO 54 I=1,15
0010            DO 55 J=1,15
0011            P(I,J)=0.0
0012         55 CONTINUE
0013         54 CONTINUE
0014            P(15,15)=1.0
0015            P(1,15)=U
0016            P(2,15)=1.5*U**2-.5
0017            P(2,1)=3.*U*T
0018            P(2,2)=3.*T**2
0019            DO 56 I=3,14
0020            P(I,15)=((2*I-1)*U*P(I-1,15)-(I-1)*P(I-2,15))/I
0021            P(I,I)=(2*I-1)*T*P(I-1,I-1)
0022            KA=I-1
0023            P(1,1)=P(I-2,1)+(2*I-1)*T*P(I-1,15)
0024            DO 57 J=2,KA
0025            P(I,J)=P(I-2,J)+(2*I-1)*T*P(I-1,J-1)
0026         57 CONTINUE
0027         56 CONTINUE
0028            APNU=0.
0029            APSI=0.
0030            DO 85 N=2,13
0031            DO 86 M=1,N
0032            MA=M
0033            MB=M
0034         99 PSI=(C(N,M)*COS(MA*ALONG)+S(N,M)*SIN(MA*ALONG))*((N+1)*P(N,MB)*U-(
               1N-MA+1)*P(N+1,MB))
0035            PNU=MA*P(N,MB)*(C(N,M)*SIN(MA*ALONG)-S(N,M)*COS(MA*ALONG))
0036            APSI=APSI+PSI
0037            APNU=APNU+PNU
0038            IF(M.EQ.14) GO TO 85
0039         86 CONTINUE
0040            M=14
0041            MA=0
0042            MB=15
0043            GO TO 99
0044         85 CONTINUE
0045            PPSI=+APSI*3600.0/(T*0.017453293)
0046            PPNU=-APNU*3600.0/(T*0.017453293)
0047            WRITE(6,38)PPSI,PPNU
0048         38 FORMAT(5X,'THE DEFLECTION IN THE MERIDIAN IS',F9.3//5X,'THE DEFLEC
               1TION IN THE PRIME VERTICAL IS',F9.3///)
0049            STOP
0050            END
```

APPENDIX C

PHYSICAL LIBRATION EQUATIONS

As stated by Kolaczek [14], physical libration is the physical deviation of the moon's motion from that described by Cassini's Laws. It can be treated as perturbations on the elements of the lunar orbit and rotation. Thus, the three components are called libration in longitude τ, in node σ, and in inclination ρ. The libration in longitude is a perturbation on the celestial longitude of the moon (can be considered as a correction to lunar time), libration in node on the celestial longitude of the node, and libration in inclination on the inclination I of the moon's equator. These perturbations are small, never exceeding 2' of arc. They can be expressed as follows:

$$\tau = \Sigma a_i \sin(ng + mg' + pF + qD)$$

$$I\sigma = I\tau + \Sigma b_i \sin(ng + mg' + pF + qD)$$

$$\rho = \Sigma c_i \cos(ng + mg' + pF + qD)$$

Where g and g' are the mean anomaly of the moon and sun respectively (dependent on time).

$$F = g + w$$

$$D = g - g' + w - w'$$

Where w and w' are the arguments of the perigrees of the moon and sun (dependent on time), n, m, p, and q and the coefficients a, b, and c are given in Table 11.

Symbols	Series	Argument Multipliers				Coefficients in Arc Seconds
		n	m	p	q	
τ	sin	0	0	2	-2	a_1 = + 1.7
		0	1	0	0	+ 91.7
		1	-1	0	-1	- 1.2
		1	0	0	-2	+ 4.2
		1	0	0	-1	- 3.5
		1	0	0	0	- 16.9
		2	-1	0	-2	+ 1.0
		2	0	-2	0	+ 15.3
		2	0	0	-2	+ 10.0
$I\sigma$	sin	0	0	2	-2	b_1 = - 3.2
		0	0	2	0	- 10.6
		1	0	-2	0	- 23.8
		1	0	0	-2	+ 2.5
		1	0	0	0	-100.7
ρ	cos	0	0	2	-2	c_1 = - 3.2
		0	0	2	0	- 11.0
		1	0	-2	0	+ 23.9
		1	0	0	-2	- 1.9
		1	0	0	0	- 98.5

Table 11. - Physical Libration Argument Multipliers and Coefficients

APPENDIX D

BLACKSHEAR SPHERICAL HARMONIC COEFFICIENTS

Table 12 below gives the C and S coefficients as determined by Blackshear in 1969. The coefficients are to the 13th order and degree. These coefficients are connected with satellite dynamics, with the potential V written in the form [9]:

$$V = \frac{Km}{r} \left\{ 1 - \sum_{N=1}^{\infty} \sum_{M=0}^{N} \left(\frac{a}{r}\right)^N \left[J_{NM} R_{NM} (\Theta, \lambda) + K_{NM} S_{NM} (\Theta, \lambda) \right] \right\}$$

N	M	C	S
0	0	1.0000573591E+00	0.
2	0	-2.0707075166E-04	0.
3	0	-6.3026014218E-06	0.
4	0	1.9378612685E-05	0.
5	0	-7.4593773641E-06	0.
6	0	-1.0784697393E-06	0.
7	0	2.4083809155E-05	0.
8	0	-2.6548898776E-05	0.
9	0	-1.5429544143E-06	0.
10	0	5.6344945025E-05	0.
11	0	-2.4602196863E-05	0.
12	0	3.2989171030E-05	0.
13	0	-5.7723614632E-05	0.
2	1	-4.4251194184E-07	-4.5725447265E-06
3	1	2.4370024362E-05	2.3006376707E-06
4	1	-5.7323804405E-06	6.8017765237E-06
5	1	1.3607744245E-06	-1.2107811323E-06
6	1	-3.6076874485E-07	2.4894914102E-06
7	1	7.8250002876E-06	8.0724355222E-06
8	1	3.9152106632E-06	-1.9291370252E-06
9	1	3.1134712059E-06	-5.3380386547E-06
10	1	9.8656663114E-07	-4.3869907744E-06
11	1	-3.0181405386E-06	-1.1622913969E-05
12	1	-7.4916591513E-06	1.7411943335E-06
13	1	-1.2121962226E-06	-5.7584594581E-06

Table 12. - Blackshear Coefficients

6	6	-2.0267463326E-09	3.8994163212E-09
7	6	-1.0459807494E-09	-3.0269761767E-10
8	6	-3.2667897321E-10	-8.8897882759E-10
9	6	1.7328428254E-10	3.2542881147E-10
10	6	9.5482215370E-11	6.0650090402E-11
11	6	4.3477571496E-11	-1.7188426198E-11
12	6	4.2482886078E-11	3.7270134398E-11
13	6	4.3675068968E-12	-1.5336991203E-11
7	7	1.2026816779E-10	-3.2283006465E-10
8	7	6.0188786284E-11	3.5932703797E-11
9	7	-1.8023550339E-11	1.0561081783E-10
10	7	-1.6122513843E-11	-2.3325805068E-11
11	7	-3.0064578083E-12	-1.0710145347E-11
12	7	-1.5484033273E-12	-2.3107720838E-12
13	7	-1.4899022434E-12	-2.4044711145E-12
8	8	-1.7001116994E-11	3.0033533379E-11
9	8	-2.8584350275E-12	7.8834743207E-14
10	8	1.5891710805E-12	-6.5597619378E-12
11	8	1.0177719212E-12	8.6181698197E-13
12	8	1.0400719186E-13	4.4891103458E-13
13	8	-2.1168402744E-14	5.5719251933E-14
9	9	9.6176983415E-13	-1.3089134543E-12
10	9	-1.9696887071E-14	-2.1938879453E-13
11	9	-1.5682882504E-13	3.5220186268E-13
12	9	-7.0712057255E-14	-3.5534890024E-14
13	9	4.6826469874E-16	-1.9224377776E-14
10	10	-3.6774006812E-14	4.6557201126E-14
11	10	-8.1140071909E-15	1.0112926706E-14
12	10	4.9625158335E-15	-1.1362089381E-14
13	10	2.1380269179E-15	1.4722610146E-15
11	11	3.3647966771E-16	-1.1213235338E-15
12	11	7.4957632120E-17	-2.4793959309E-16
13	11	-2.0181618293E-16	1.7194186339E-16
12	12	-3.6274691633E-18	-1.5526294510E-18
13	12	-1.8762164620E-18	-8.1189021267E-18
13	13	9.5540605576E-19	-1.7059499010E-19

APPENDIX E

OPTIMUM POSITIONS FOR MINIMUM STAR COORDINATE ERRORS

Stars which yield the minimum error in transformation were found to possess the coordinates of:

Lunar Declination = 0°

Lunar Right Ascension = 0° or 180°

Thus this point will fall on the ecliptic at the position of the nodes. Figures 10 and 11 (from [16]) give the positions of these stars in earth coordinates of right ascension and declination for the time January 0.5 1971, January 0.5 1972, January 0.5 1973 and January 0.5 1974. The motion of these points is in direct relationship with the motion of the lunar nodes.

Figure 10. - Positions of Ascending Node

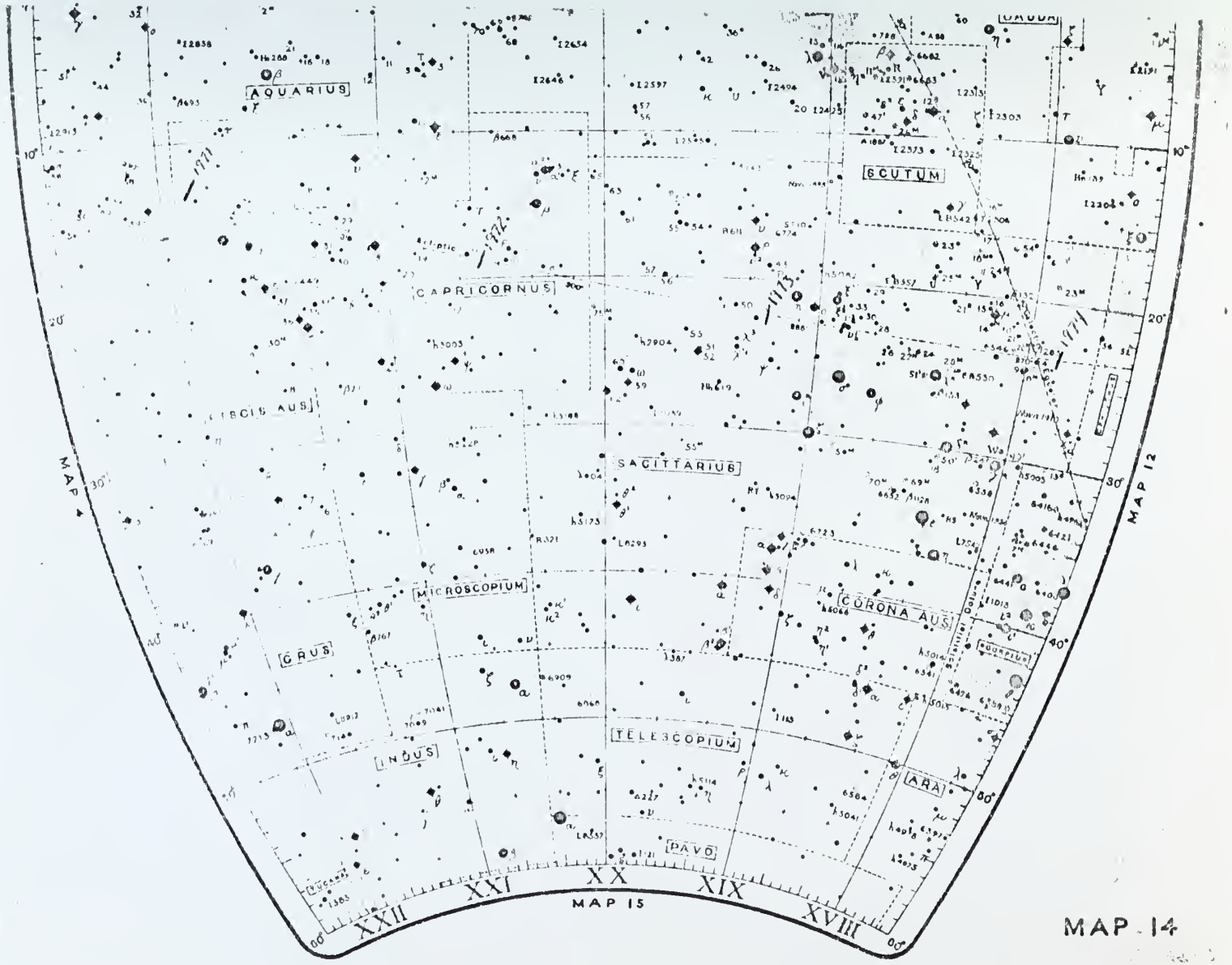

Figure 11. - Positions of Descending Node

Thesis
M247 McLean
Establishment of
selenodetic control
through measurements
on the lunar surface.
119737